PHOTOSYNTHETIC PERFORMANCE OF SINGLE-CELL C_4 SPECIES (CHENOPODIACEAE)

BY

MONICA ELIZABETH SMITH

This thesis submitted in partial fulfillment of
the requirements for the degree of

MASTER OF SCIENCE IN BOTANY

WASHINGTON STATE UNIVERSITY
School of Biological Sciences

DECEMBER 2007

To the Faculty of Washington State University:

The members of the Committee appointed to examine the thesis of MONICA ELIZABETH SMITH find it satisfactory and recommend that it be accepted

_____
Chair

_____

_____

ACKNOWLEDGEMENTS

I would like to thank my committee chair, advisor, and mentor Gerry Edwards for all his help and patience throughout this project. I would also like to thank my other committee members, Al Black and Eric Roalson, for enthusiastically serving on my committee, and making sure I made it to this point. I would like to thank Olavi Kiirats for showing me many techniques involving gas exchange measurements, and for keeping me up-to-date with foreign policy. I would like to thank Elena Voznesenskaya and Nouria Koteeva for teaching me how to grow the plants for this project. Thank you Nouria for learning how to take gas-exchange measurements with me. Thanks JoonHo Park, Valeria Lynch-Holm, and Chris Davitt for all the help in the Franceschi Microscopy and Imaging Center.

I would also like to thank my family and friends, especially my sister Melissa, for her never-ending support, encouragement, and distraction.

PHOTOSYNTHETIC PERFORMANCE OF SINGLE-CELL C_4 SPECIES

(CHENOPODIACEAE)

Abstract

By Monica Elizabeth Smith, MS
Washington State University
December 2007

Chair: Gerald E. Edwards

This study compared the light and CO_2 response curves of two single-cell C_4 species, *Bienertia sinuspersici* and *Suaeda* (formerly *Borszczowia*) *aralocaspica* (Bunge, to closely related Kranz-type C_4 species and C_3 species. The Kranz-type C_4 species were represented by *Suaeda taxifolia* (Suaedoid type) and *S. eltonica* (Conospermoid type). *Suaeda heterophylla* and *S. maritima* were the representative C_3 species; both are Brezia anatomical subtypes (Schütze, Freitag *et al.* 2003).

Photosynthetic rates were similar between the single-cell C_4 species and the Kranz-type C_4 species with *S. aralocaspica* having slightly higher assimilation rates and *B. sinuspersici* having slightly lower assimilation rates than *S. taxifolia* and *S. eltonica* on area, chlorophyll, and protein bases. However, both single-cell C_4 species had higher assimilation rates than their Kranz-type C_4 counterparts when rates were expressed on a Rubisco basis. The single-cell C_4 and Kranz-type C_4 species had similar CO_2 compensation points, saturation of photosynthesis near ambient CO_2, Rubisco to soluble protein ratio, and water use efficiency. The values for these parameters were significantly different from the C_3 species. The results suggest that the C_4

cycle is functioning efficiently in the single-cell C_4 systems, and that the single-cell C_4 mechanism may have a more efficient Rubisco enzyme than the Kranz-type C_4.

TABLE OF CONTENTS

Page

LIST OF TABLES

LIST OF FIGURES

DEDICATION

This thesis is dedicated to my family and close friends for always believing in me.

CHAPTER ONE

INTRODUCTION

Arguably, the most important process in the world is the conversion of light energy into chemical energy, otherwise known as photosynthesis. Of the organisms capable of photosynthesis, plants are the most diverse, economically, and ecologically important. Life as we know it is highly dependent on photosynthesis from plants for oxygen, food, fiber, fuels, medicines, etc. Currently, three main modes of photosynthesis have been recognized in terrestrial plants: C_3, Crassulacean acid metabolism (CAM), and C_4. All three modes of photosynthesis are defined by the mechanism by which Rubisco (ribulose-1, 5-biphosphate carboxylase oxygenase) acquires CO_2 for the first reaction in the Calvin-Benson cycle.

C_3 photosynthesis is the simplest and most common mode of photosynthesis. In C_3 photosynthesis, atmospheric CO_2 is directly assimilated by Rubisco. It is called C_3 because the first stable organic product of CO_2 assimilation is a three-carbon molecule, 3-phosphoglycerate (3-PGA) (Taiz and Zeiger 1998).

CAM is most prevalent in succulent desert plants and epiphytes. It is characterized by nocturnal uptake and fixation of CO_2 by phospho*enol*pyruvate carboxylase (PEPC) into oxaloacetate (OAA), which is then reduced to malate. The malate is stored in large central vacuoles until the subsequent light period. During the day, malate is decarboxylated to supply CO_2 to Rubisco. This pathway is named after the first plant family that it was discovered in, Crassulaceae, and the high diurnal fluctuation in acidity is due to the change in malate concentration. This modification in photosynthesis has a major advantage for plants with

minimal water availability by allowing the stomata to close during the hottest part of the day, thus reducing water loss via transpiration (Edwards and Walker 1983).

Of the three different modes of photosynthesis, C_4 has the fewest species; but those few species are highly productive. It is estimated that C_4 plants contribute about 30% of the terrestrial productivity on Earth, dominating tropic and subtropic regions (Edwards *et al.* 2004; Sage 1999). Similar to CAM, CO_2 is initially fixed by PEPC in C_4 photosynthesis. However, unlike CAM that temporally separates the initial fixation phase from the Calvin-Benson cycle, C_4 metabolism spatially separates the two different phases. During the day, CO_2 is fixed by PEPC in one compartment where Rubisco is absent, and then the organic acid serves as a donor of CO_2 as it is transported into a compartment that contains Rubisco (Edwards and Walker 1983).

Different mechanisms have evolved to donate CO_2 to Rubisco as a compensation for the effects of high levels of oxygen in the atmosphere on the enzyme. High levels of oxygen are a problem for plants because Rubisco has a propensity to react with oxygen (O_2) as well as carbon dioxide (CO_2). The oxygenase reaction leads to a process known as photorespiration which results in the consumption of adenosine triphosphate (ATP) and reductant power, and the loss of CO_2 (Edwards and Walker 1983). The C_4 pathway in terrestrial plants eliminates photorespiration, or suppresses it considerably, by concentrating CO_2 around Rubisco. The C_4 pathway achieves this by initially fixing CO_2 into an organic acid by PEPC, which lacks an oxygenase activity. The product of this reaction is OAA, which is immediately converted into either malate or asparate. The C_4 acids are then transported from the site of fixation to another compartment that contains Rubisco and decarboxylated to release CO_2. C_4 species are categorized into three different sub-types based on the type of decarboxylation enzyme; NAD-malic enzyme (NAD-ME), NADP-malic enzyme (NADP-ME), and phospho*enol*pyruvate

carboxykinase (PEP-CK) Pyruvate is generated as a result of the decarboxylation reactions in NAD-ME and NADP-ME sub-types; phospho*enol*pyruvate is generated as the result of decarboxylation reaction in PEP-CK sub-type (Taiz and Zeiger 1998). Pyruvate use to generate more phosphoenolpyruvate (PEP) via the enzyme pyruvate orthophosphate dikinase (PPDK), where PEP can then be used by PEPC to fix another CO_2 molecule. This increases the concentration of CO_2 around Rubisco, and suppresses the oxygenation reaction (Edwards and Walker 1983). Figure 1 diagrams how CO_2 is "pumped" into the Rubisco containing compartment in Kranz-type C_4 plants.

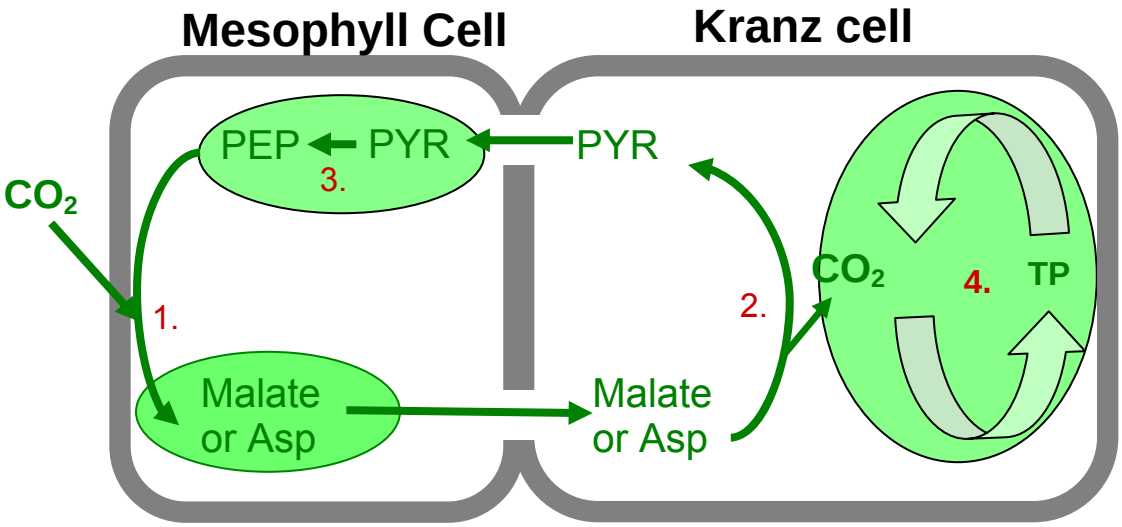

Figure 1. Schematic of the C_4 cycle. CO_2 is initially fixed in one compartment by PEPC and transported to another compartment as malate or aspartate where it is fixed by the Rubisco in the Calvin-Benson cycle. Enzymes: 1. PEPC, 2. CO_2 releasing enzymes (NAD-ME, NADP-ME, or PEP-CK), 3. PPDK, 4. Calvin-Benson cycle. Abbreviations: Asp – aspartate, TP – Triose phosphate, PYR – pyruvate, PEP – phospho*enol*pyruvate.

History

Evidence suggests that when Rubisco first evolved in photosynthetic bacteria, approximately 3 billion years ago, the CO_2 levels in the atmosphere were considerably higher (~

100-fold higher) and the O_2 levels were significantly lower than they are today (Edwards *et al.* 2004). Therefore, during the evolution of Rubisco there was not a strong natural selection against the oxygenase activity, which is considered an unavoidable consequence of the catalytic mechanism of Rubisco (Edwards and Walker 1983; Edwards *et al.* 2004; Sage 2002).

Approximately 65 million years ago, during the Tertiary period, CO_2 levels dropped low enough that photorespiration could have driven the evolution of several different forms CO_2 concentrating mechanisms (CCMs). CCMs are an important component in C_4 photosynthesis that reduces the rate of photorespiration by concentrating CO_2 around Rubisco (Edwards *et al.* 2001b). Since then it is estimated that C_4 photosynthesis has arisen as many as 40 to 50 times in terrestrial plants (Edwards *et al.* 2004).

In order for C_4 photosynthesis to function efficiently there needs to be: (1) a spatial separation between the initial site of CO_2 fixation by PEPC and the compartment containing Rubisco; (2) dimorphic chloroplasts with site specific expression of Rubisco; (3) a barrier against CO_2 diffusion out of the compartment with Rubisco; and (4) site specific increase in C_4 enzymes (Edwards *et al.* 2001b; von Caemmerer and Furbank 2003).

Kranz anatomy was first described in the late 1800's by Gottlieb Haberlandt. Haberlandt noticed some plants in the plant families Poaceae and Cyperaceae had unusual leaf anatomy with increased frequency of vascular bundles and large bundle sheath cells with a high concentration of chloroplast surrounded by mesophyll cells (Edwards *et al.* 2004). This unique anatomical design was coined Kranz anatomy, for the wreath-like chlorenchyma surrounding the vascular bundles.

The C_4 pathway was initially discovered in the 1950's and 1960's by a few scientists who performed experiments with radioactive CO_2 on maize and sugarcane, either by feeding $^{14}CO_2$

and analyzing products or performing the pulse-chase experiments with $^{14}CO_2$ followed by non-radiolabeled CO_2 from the atmosphere (Hatch 2002). The methods used were similar to those of Calvin and Benson who elucidated the Photosynthetic Carbon Reduction cycle (PCR) from studies on Chlorella and other higher plants (Hatch and Slack 1966; Hatch and Slack 1970; Kortschack *et al.* 1965). These scientist saw that the first labeled products were malate and aspartate, instead of 3-phosphoglycerate (3-PGA) (Hatch 2002). It became obvious that some plants used a different strategy than the PCR cycle for fixing CO_2. However, the reason for this unique pathway did not become clear until the oxygenase activity of Rubisco and photorespiration were elucidated in the late 1960's to the early 1980's (Bowes *et al.* 1971; Forrester *et al.* 1966; Ögren and Bowes 1971). Since then, many among 19 families have been identified as having the C_4 photosynthetic pathway, and until recently all known examples of any terrestrial plants with C_4, photosynthesis had some form of Kranz anatomy (Akhani *et al.* 2005; Edwards and Walker 1983; Edwards *et al.* 2004; Freitag and Stichler 2000; Voznesenskaya *et al.* 2002; Voznesenskaya *et al.* 2001).

Identifying characteristics of C_4 species

C_4 species are identified by several distinct characteristics based on anatomy, enzymology, and physiology. Kranz anatomy has been a used as a convenient method to screen for C_4 photosynthesis since no other photosynthetic pathway, C_3 or CAM, exhibits Kranz anatomy (Edwards and Walker 1983). Another common test to identified C_4 photosynthesis is by $\delta^{13}C$ discrimination values. In C_3 species, Rubisco preferentially reacts with the $^{12}CO_2$ isotope over the $^{13}CO_2$ isotope, which results in an enriched ^{12}C isotope composition. However, in C_4 plants PEPC does not discriminate between ^{13}C and ^{12}C, which results in C_4 plants having a

higher $^{13}C/\ ^{12}C$. The problem with this method is that C_4 plants cannot be distinguished from obligate CAM plants using this method. Many CAM plant have the same $\delta^{13}C$ discrimination values as C_4 plants since in both forms of photosynthesis atmospheric CO_2 is initially fixed by PEPC (Bender 1971; Edwards and Walker 1983).

Enzymatic assays, western blots, and immunolocalization have frequently been used to test for the expression levels of enzymes necessary for the C_4 cycle, i.e. PEPC, and PPDK, and to identify C_4 species (Edwards and Walker 1983; Edwards *et al.* 2001a). Immunolocalization is also useful to determine in which compartments photosynthetically important enzymes are being expressed (Edwards *et al.* 2001a). In most C_4 species, Rubisco is only expressed in the bundle-sheath cells, whereas high levels of PEPC and PPDK are generally only expressed in the mesophyll cells (Edwards and Walker 1983).

Finally, the rate of photosynthesis in C_4 plants under different environmental conditions is distinct from that of C_3 plants (Edwards and Walker 1983). Most notably, C_4 photosynthetic rates are not inhibited by ambient levels of O_2 (approx. 21%), whereas the photosynthetic rates of C_3 plants is considerably reduced by 21% O_2, especially at low CO_2 levels. As seen in Figure 2, C_4 plants also have a CO_2 compensation point that is near zero and their photosynthetic rate is nearly saturated at

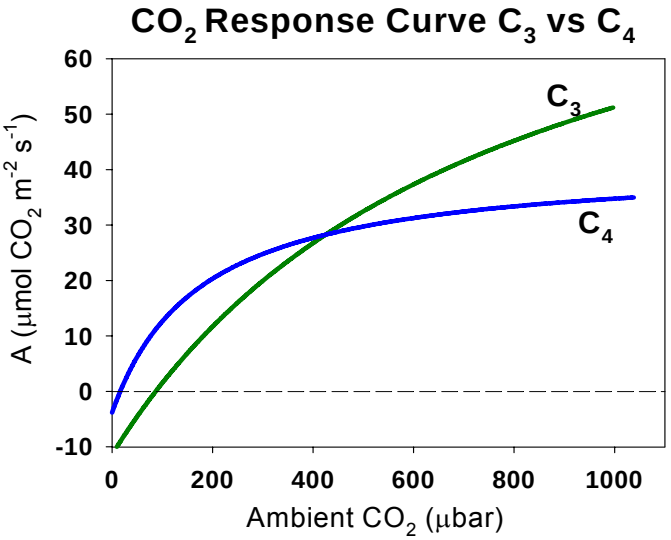

Figure 2. Typical CO_2 response of C_3 and C_4 species.

ambient levels of CO_2 (approx. 340 µbar). Whereas C_3 plants have a CO_2 compensation point typically between 40 and 100 µbar CO_2 (dependent on temperature) and their photosynthetic rate doesn't approach saturation until the levels of CO_2 are increased two to three fold above current atmospheric levels (see typical CO_2 response curve in Figure 2) (Edwards and Walker 1983).

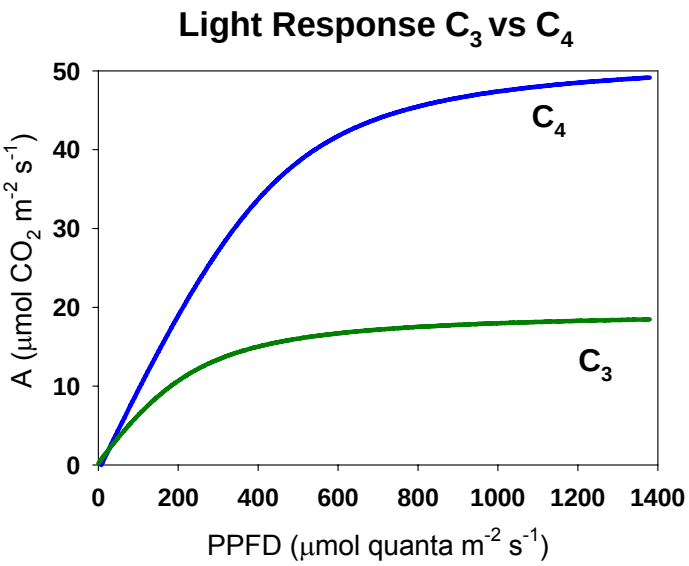

Figure 3. Light response typical for C_3 and C_4 species.

C_4 species also typically have a higher maximum rate of photosynthesis and require more light to reach photosynthetic capacity, than their C_3 counterparts (as illustrated in Figure 3) (Ehleringer and Pearcy 1983). Under moderate temperatures, the quantum yield is similar between C_3 and C_4 species. However, the quantum yield of C_3 photosynthesis is highly dependent on temperature, increasing in cooler temperatures and decreasing under in hot temperatures. In contrast, the quantum yield of C_4 species is relativity unaffected by temperature with a crossover point between C_3 and C_4 around 25˚C (Berry and Björkman 1980; Björkman and Berry 1973).

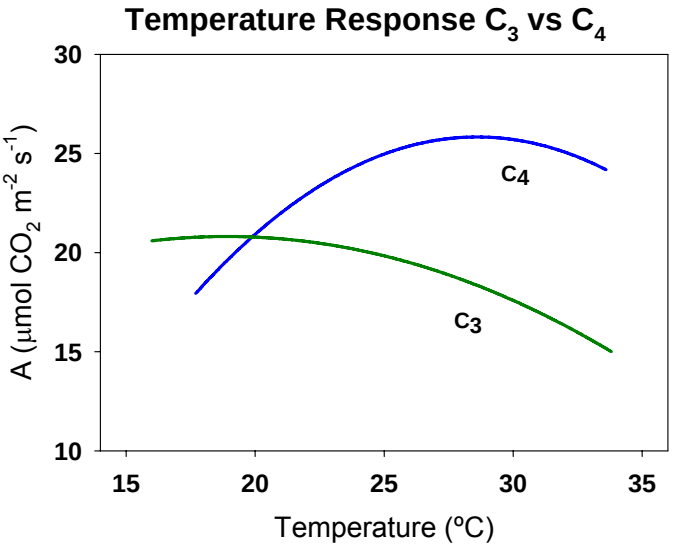

Figure 4. Temperature responses typical of C_3 and C_4 species.

Temperature by itself is useful in distinguishing between C_3 and C_4 photosynthetic types (Fig. 4). As temperature increases so does the Rubisco oxygenase activity, resulting in an increase in photorespiration and a decrease in the net photosynthetic rate in C_3 species (see Fig. 4). In C_4 species, the temperature optimum is typically higher than that in C_3 plants because the CCM of the C_4 mechanism reduces photorespiration (Berry and Björkman 1980; Björkman and Berry 1973; Edwards and Walker 1983).

Breaking the Dual-Cell Paradigm

Recently the discovery of three species, *Suaeda* (formerly *Borszczowia*) *aralocaspica* (Bunge) Freitag and Schütze (2003), *Bienertia cycloptera* Bunge ex Boiss, and *B. sinuspersici* Akhani, in family Chenopodiaceae have challenged the three decade old paradigm that Kranz-anatomy is required for C_4 photosynthesis in terrestrial plants (Akhani *et al.* 2005; Kapralov *et al.* 2006; Schütze *et al.* 2003). These three species represent two unique strategies to carry out C_4 photosynthesis within a single chlorenchyma cell. They have an unusual cellular ultra-structure for spatial separation of function of C_4 photosynthesis between two cytoplasmic compartments (Edwards *et al.* 2004). There is extensive development of the cytoskeleton, with microtubules being essential in maintaining organelle positioning within the chlorenchyma cell (Chuong *et al.* 2006). The development of these specific chlorenchyma anatomies is dependent on developmental and environmental signaling, and may be controlled by nuclear directed partitioning of organelles into separate compartments with biochemical and ultrastructural changes (Voznesenskaya *et al.* 2005). The following is a brief overview of the discovery of these unique systems.

Suaeda aralocaspica

As part of a larger systematic study of leaf anatomy in Salsoloideae, a subfamily of Chenopodiaceae, Freitag and Stichler (2000) found the unusual chlorenchyma cells of *Suaeda*. The leaf anatomy of *S. aralocaspica* is arranged so that beneath the epidermis and hypodermis layers is a single layer of tightly packed chlorenchyma cells that surround water storage cells and vascular bundles. The chlorenchyma cells are elongated with chloroplasts polarized to opposite ends of the cell. The proximal end has a high density of chloroplasts with large starch granules. The distal end contains a few small chloroplasts that lack starch grains. The chlorenchyma cells are tightly packed together with intercellular air space only at the distal end. The elongated cells so closely resemble the Kranz anatomy of other closely related C_4 species that the authors of the first paper describing the internal leaf anatomy of *S. aralocaspica* said that the lack of periclinal walls might be easily overlooked in thick sections with low resolution. This type of anatomy, with elongated chlorenchyma cells with chloroplasts polarized to either end of the end, was named borszczoviod by Freitag and Stichler (2000) and later renamed *Borszczowia* type non-Kranz C_4 anatomy after the (Schütze *et al.* 2003).

In addition to the anatomical similarity to closely related Kranz-type C_4 species, the $\delta^{13}C$ values are in a range that is typical of C_4 or CAM. With this information, Freitag and Stichler (2000) proposed that this plant might perform C_4 photosynthesis without a cell wall separating the two compartments.

Subsequent immunolocalization and western blot assays have demonstrated the expression of C_4 enzymes, with Rubisco located only in the proximal end, and PPDK only in the distal end (Voznesenskaya *et al.* 2001). PEPC is located throughout the cytoplasm, which could result in futile cycling if active near the site of decarboxylation. However, PEPC may be less

active in the proximal region due to lack of substrate (PEP), since PPDK expression is only at the distal end. Inhibition and/or phosphorylation by malate in the distal region may regulate the expression of PEPC in that region. It is also possible that PEPC protein levels in the distal region will be very low due to limited cytosolic space in this region (Lara *et al.* 2006).

Immunolocalization and electron microscopy showed dimorphic chloroplasts in the proximal end and the distal end. Chloroplasts are dimorphic based on starch content, enzymes composition, and thylakoid development. The chloroplasts in the proximal end have more grana and starch grains than the distal chloroplasts. The distal chloroplasts lack Rubisco but have high levels of PPDK, whereas the proximal chloroplast have Rubisco but have low amounts of PPDK. Mitochondria are located in the proximal end of the cell. These mitochondria contain NAD-ME, which decarboxylated malate, releasing CO_2 for fixation by Rubisco.

Pulse-chase experiments with $^{14}CO_2$ revealed malate and asparate to be the first labeled products (Voznesenskaya *et al.* 2003). All this evidence indicates either a C_4 or CAM mode of photosynthesis, but a test of titratable acidity showed no diurnal fluctuation, which would be characteristic of CAM (Edwards *et al.* 2004). The previous results, in conjunction with physiological data that shows that photosynthesis in not inhibited by the presence of O_2 at low CO_2 concentrations indicated this is a fully functional C_4 system (Voznesenskaya *et al.* 2003).

Bienertia cycloptera* and *B. sinuspersici

The genus *Bienertia* Bunge consists of two species, *Bienertia cycloptera* Bunge ex Boiss. and *B. sinuspersici* (Akhani et al. 2005). Both species differ in overall plant size, habitat range, leaf shape, flowering time, number of chlorenchyma layers, and karyotype (Akhani *et al.* 2005). Despite these differences, *B. sinuspersici* was only recently recognized as a separate species

from *B. cycloptera* (Akhani *et al.* 2005). The two species do share a single-cell C_4 photosynthetic pathway distinct from *S. aralocaspica* (Akhani *et al.* 2005; Freitag and Stichler 2002). The succulent leaves of *Bienertia* species have a tightly connected epidermis, 2-3 layers of loosely packed chlorenchyma cells with exposure to intercellular airspace on all sides, and large water storage cells surrounding the vascular bundles. The chlorenchyma cells of *Bienertia* species have a central cytoplasmic compartment (CCC) with a dense ball of chloroplasts and mitochondria, and a thin layer of cytoplasm with small chloroplasts around the periphery (Akhani *et al.* 2005; Freitag and Stichler 2002; Voznesenskaya *et al.* 2002). A single large vacuole and several cytoplasmic channels separate the two compartments from each other (Park, unpublished data). The peripheral chloroplasts are similar to the chloroplasts found in mesophyll cells in Kranz-type C_4 plants; they lack Rubisco, are deficient in granal stacking, and lack starch grains. The chloroplasts in the CCC are typical of chloroplasts found in bundle sheath cells, with lots of granal stacking, and starch grains (Akhani *et al.* 2005; Freitag and Stichler 2002; Voznesenskaya *et al.* 2002). Chloroplasts in the CCC are also in close proximity with mitochondria, and since the C_4 acid is decarboxylated in the mitochondria by NAD-ME, this functions to donate CO_2 to Rubisco in the adjacent chloroplasts (Voznesenskaya *et al.* 2002). This new leaf anatomy is called bienertioid (Freitag and Stichler 2002). Recently Schütze *et al*. (2003) renamed this anatomy *Bienertia* type non-Kranz C_4 anatomy.

In its native habitat, *Bienertia* species have $\delta^{13}C$ isotope discrimination values in the range of C_4/ CAM plants (Akhani *et al.* 2005; Akhani *et al.* 1997; Freitag and Stichler 2002). Assays for titratable acidity showed no major diurnal fluctuations, which indicate it is functioning as a C_4 plant rather than a CAM plant (Edwards *et al.* 2004; Voznesenskaya *et al.* 2002). In addition, photosynthetic studies have shown that O_2 does not inhibit *Bienertia.* In fact,

it appears *Bienertia* has an increase in photosynthetic capacity under 21% O_2 versus 2% O_2 (Voznesenskaya *et al.* 2002).

Like *S. aralocaspica*, *Bienertia* shows a spatial separation of Rubisco, NAD-ME, and PPDK. Also like *S. aralocaspica*, PEPC is located throughout the cytoplasm, and is suggested to be controlled in a similar manner to *S. aralocaspica* and other Kranz-type C_4 plants (Lara *et al.* 2006). It has been suggested that perhaps *Bienertia* may have some flexibility in its photosynthetic pathway; it may be able to switch between C_4 and C_3, or C_4 and CAM (Edwards *et al.* 2004; Freitag and Stichler 2002). However, there is currently no evidence available to support this claim.

How to define C_4 species now

The lack of Kranz-anatomy can no longer be used to exclude a plant from being C_4. Despite this, anatomy is still important in the screening for potential C_4 species. The distribution of intercellular air space and the specific partitioning of organelles within the chlorenchyma cell are vital for the C_4 cycle to function in both *Borszczowia* and *Bienertia* type anatomies. The lack of intercellular air space in *S. aralocaspica* at the proximal end reduces the possibility of gases (CO_2 and O_2) diffusing to that area of the cell and reacting with Rubisco first or leakage of CO_2 from the cell following decarboxylation of malate, thus reducing the possibility of photorespiration. *Bienertia* does not require such specific restriction of intercellular air space since all Rubisco containing chloroplasts are in the CCC. Having Rubisco located only in the CCC creates a long diffusive path for gases to reach Rubisco, and CO_2 must diffuse first through the peripheral cytoplasm with highly active PEPC before reaching the CCC. In conclusion,

anatomy still plays an important role in the function and discovery of C_4 photosynthesis, and in considering criteria for identifying additional C_4 species.

Questions remaining

Despite the evidence that *S. aralocaspica* and *Bienertia* species have single-cell C_4 photosynthesis, many questions remain. The most prominent questions concerning the validity of these species as fully functional C_4 plants are: (1) how is the spatial separation of the two cytoplasmic compartments controlled, (2) are there conditions where this not maintained, (3) how is CO_2 leakage from the site of C_4 acid decarboxylation prevented, (4) is the C_4 cycle as efficient as the Kranz-type systems, and (5) what was the driving force in single-cell C_4 evolution?

In this thesis, I have employed gas-exchange techniques to analyze features of CO_2 fixation, Rubisco content, and water-use efficiency in comparison with closely related Kranz-type C_4 and C_3 species in an effort to answer some of the questions about the functionality of single-cell C_4 photosynthesis.

CHAPTER TWO

PHOTOSYNTHETIC PERFORMANCE OF SINGLE-CELL C_4 SPECIES, *BIENERTIA SINUSPERSICI* AND *SUAEDA ARALOCASPICA* (CHENOPODIACEAE)

Introduction

The relative efficiency of C_4 photosynthesis compared to C_3 photosynthesis under CO_2 limiting conditions is highly dependent on the effectiveness of the CO_2 concentrating mechanism around Rubisco. The leakage of CO_2 from the RuBP-carboxylase compartment would result in futile cycling and lower photosynthetic efficiency of the C_4 cycle (von Caemmerer and Furbank 2003). Typical Kranz-type C_4 species prevent futile cycling and leakiness by employing a dual cell system, which spatially separates the initial carboxylation and decarboxylation steps into separate cells. For a long time, Kranz anatomy was thought to be essential to the function of C_4 photosynthesis (Edwards *et al.* 2004; Sage 2002; Voznesenskaya *et al.* 2002; Voznesenskaya *et al.* 2001).

Recently, three species, *Suaeda aralocaspica* (Bunge) Freitag and Schütze (formally *Borszczowia*), *Bienertia cycloptera* Bunge ex Boiss. and *B. sinuspersici* Akhani (Kapralov *et al.* 2006; Schütze *et al.* 2003) (Chenopodiaceae subfamily Suaedoideae) were discovered to carry out C_4 photosynthesis within a single photosynthetic cell (Akhani *et al.* 2005; Freitag and Stichler 2000; Freitag and Stichler 2002; Voznesenskaya *et al.* 2002; Voznesenskaya *et al.* 2001). *Suaeda aralocaspica* carries out C_4 photosynthesis within a single elongated chlorenchyma cells with the initial CO_2 fixation by phospho*enol*pyruvate carboxylase (PEPC) at the distal end, and decarboxylation by NAD-ME and fixation by Rubisco at the proximal end (Voznesenskaya *et al.* 2001). *Bienertia cycloptera* and *B. sinuspersici* have another novel means of conducting C_4 photosynthesis within a single-cell that is different from *S. aralocaspica.*

Bienertia separates the C_4 and the C_3 cycles between the periphery of the cell and the central cytoplasmic compartment located in the center of the cell; the initial site of CO_2 fixation at the periphery by PEPC, and the C_4 acid decarboxylation/Rubisco fixation in a ball-like central cytoplasmic compartment (Voznesenskaya *et al.* 2002).

The discovery of two unique cell types that exhibit C_4 photosynthesis characteristics within three species of Chenopodiaceae has proven that terrestrial C_4 photosynthesis does not require Kranz anatomy (Akhani *et al.* 2005; Freitag and Stichler 2002; Voznesenskaya *et al.* 2002; Voznesenskaya *et al.* 2001). However, the photosynthetic performance of the single-cell C_4 species has never been compared to Kranz-type or C_3 species under varying environmental conditions. In C_4 species, anatomical and biochemical features of photosynthetic tissues are important for efficient carbon acquisition under CO_2 limiting conditions such as drought, high temperatures, high light, and salinity (von Caemmerer and Furbank 2003). The family Chenopodiaceae has the highest number of C_4 species among eudicots with great diversity of structure, and biochemical subtypes. Within Chenopodiaceae, five different types of C_4 Kranz-anatomy have been identified, atriplicoid, Kranz-halosarcoid, kochioid, salsoloid, and Kranz-suaedoid, and two different decarboxylation subtypes, NAD-ME and NADP-ME (Akhani *et al.* 1997; Freitag and Stichler 2000; Kapralov *et al.* 2006; Schütze *et al.* 2003; Voznesenskaya *et al.* 2001).

In this study, photosynthetic performance of single-cell C_4 species, *S. aralocaspica* and *B. sinuspersici,* were compared with closely related representatives of C_4 Kranz-type and C_3 species from the subfamily Suaedoideae. *Suaeda taxifolia* Standley and *S. eltonica* Iljin represent two different Kranz-types, suaedoid and conospermoid respectfully (Schütze *et al.* 2003). *Suaeda heterophylla* Bunge (sect. *Brezia*) and *S. maritima* Dumort. (sect. *Brezia*) represent the C_3

photosynthetic types (Akhani *et al.* 1997; Kapralov *et al.* 2006; Schütze *et al.* 2003). The representative photosynthetic types in subfamily Suaedoideae have succulent, semi-terete leaves with water storage tissue surrounding the vascular bundles. C_4 species in this subfamily are biochemical NAD-malic enzyme subtype (Voznesenskaya *et al.* 2007). Species-dependent differences in CO_2 compensation point, CO_2 fixation in response to varying light and CO_2 maximum photosynthetic rates, and water use efficiency were measured to compare the photosynthetic performances of the species in this study. The objective was to compare the efficiency of single-cell C_4 photosynthesis versus Kranz-type C_4 and C_3 photosynthesis in closely related species.

Methods and Materials

Plant material.

Suaeda aralocaspica and *S. maritima* seeds were germinated on moist paper towels in Petri dishes. After the radical appeared, *S. aralocaspica* seeds were transferred to a soil mixture of 1 part potting soil, two parts sand, 0.25 part gypsum, 0.5 part Perlite, and 0.5 part clay. All other species were propagated from cuttings in rooting MS media (4.3 g/L complete MS salt (Plant Media),10 ml/L 100X MS vitamin stock, 20 g/L sucrose for 2MS, 1.95 g/L MES buffer (10 mM MES free acid), 10 mM – 0.5844 g/L, pH 5.8, and 0.8 % agar/gelrite). After root formation, the cuttings were transferred to soil media, and gradually exposed to increasing light and decreasing humidity. *Bienertia sinuspersici* was grown in a soil mixture of 1 part potting soil, and 0.5 parts of each of the following: sand, gypsum, and clay. All other species were grown in regular potting soil.

Plants were grown in a growth chamber (model GC-16; Enconair Ecological Chambers Inc., Winnipeg, Canada) under maximum photosynthetic flux density (PPFD) of 400 µmol quanta m^{-2} s^{-1} during a 14/10 h, 25 /18 ºC day/night cycle, atmospheric CO_2 and 50% relative humidity. The lights in the chamber were programmed to come on and off gradually through a stepwise increase or decrease over a two h period at the beginning and end of the photoperiod respectively.

Gas exchange.

Rates of photosynthesis and transpiration were measured with an LCpro+ portable infrared CO_2 gas analyzer from ADC BioScientific Ltd, England at varying light intensities and CO_2 concentrations. Photosynthetic rates were expressed per unit leaf area, mg chlorophyll, mg soluble protein, and mg Rubisco. Induction time was measured prior to gas-exchange measurements. The plants were removed from the chamber and placed in the dark for 1 h to deactivate the photosynthetic apparatus. After dark adaptation, a branch of the plant was placed inside the conifer chamber with conditions under 1000 PPFD, 25 ˚C, 340 µbar CO_2, and 12 mbars vapor pressure until a steady state rate of photosynthesis was achieved. Light response measurements were made in decreasing intervals of 4 min from a maximum PPFD of 1777 µmol quanta m^{-2} sec^{-1} down to 0 µmol quanta m^{-2} sec^{-1}, and then in increasing intervals of 10 min from 0 to 1777 µmol quanta m^{-2} sec^{-1}. There was no significant difference between the curves generated whether the sequence was from high to low light followed by low to high light, or vice versa. Due to time constraints, it was adopted as standard procedure to measure light response curves after light induction from high light decreasing to low light.

The rate of photosynthesis with varying ambient levels of CO_2 (A/ Ca response curves) were generated by gradually decreasing external CO_2 concentrations from ambient (~340 µbar) to approximately 5 µbar CO_2. External concentrations were then gradually increased from 5 µbar to 927 µbar CO_2 and then decreased to 340 µbar. From these curves the CO_2 compensation point, carboxylation efficiency (C_E), and CO_2 levels required for saturating the rates of photosynthesis were estimated. The intercellular levels of CO_2 (Ci) values were calculated but not used in the graphical representation because of some instability in the instrument's H_2O vapor readings which gave less consistent results.

The CO_2 compensation point was measured by two methods. In one case, the CO_2 compensation point (Γ) was measured by determining the zero intercept with variable CO_2 under high light. In the other method, the compensation point (Γ_*) was by the method described by Brooks and Farquahar (1985) which eliminates the contribution of dark type mitochondrial respiration to the CO_2 compensation point. Their method provides a measure of the compensation point based on Rubisco functional carboxylase versus oxygenase activity.

Water-use efficiency (WUE) was measured during steady state photosynthesis at 1000 PPFD, 25 ˚C, 12 mbars vapor pressure, and 340 µbar CO_2. This measurement was repeated 3x for each species.

Immediately after gas exchange measurements the branch was removed from the plant, weighed, and stored in liquid nitrogen.

Determination of leaf area.

The overlapping projected area was determined using Scion's ImageJ 1.36b program (Rasband 1997-2007) from a digital picture. The image was then converted into a threshold

image. The program measures the area of the black shapes using the picture scale as a reference. The overlapping projected area is typically used for calculations of 3D branches or complex leaf structures, because it is assumed that the incident surface to the light is photosynthesizing at the highest rate (Landsberg and Ludlow 1970). From here on out, the overlapping projected leaf area will be referred to as leaf area when referring to gas-exchange measurements.

Absorbed quanta was determined using a integrating sphere from Labsphere, Inc. North Sutton, NH, using two different methods described in Idle and Proctor (1983) and the Middleton *et al.* (1990). Both methods were developed to measure absorbed quanta for conifer needles. There was little difference in the values between the two methods. The following equation was used to determine absorbed quanta using the Idle and Proctor method (1983)

$$\alpha_L = 1 - \frac{(1-\alpha_S)\Phi_1 A_L}{(\Phi_1 - \Phi_2)A_S} \qquad \text{Eq. (1)}$$

Where α_L is the absorptivity of the leaf, α_S is the absorptivity of the sphere which was estimated to be around 1%, A_L is the total surface area of the leaf, and A_s is the surface area of the sphere (314 cm^2). Φ_1 and Φ_2 represent the photon flux density exiting the integrating sphere with and without the branch, respectfully. Photosynthetic photon flux density (PPFD) was measured with a quantum sensor from Li-COR model LI-189 (Lincoln, NE).

Since the lighting in the integrating sphere is uniform throughout, the non-overlapping projection area was used to calculate the total surface area (Idle DB and Proctor 1983). The non-overlapping projection area was determined by detaching all the leaves from the branch and laying them out flat. Scion Image was used to calculate the non-overlapping projection area as

described previously. The total surface area of the branch was determined by multiplying the non-overlapping projection area by 3.14 to account for the three dimensions of the branch.

Chlorophyll, soluble protein, and Rubisco determination.

Total chlorophyll, soluble protein, and Rubisco contents were determine from crude extracts of branches used in gas-exchange and stored in liquid nitrogen. Branches were ground with liquid N_2 in a mortar and pestle to a fine powder. The powder was homogenized in an activating extraction buffer consisting of 20 mM $MgCl_2$, 20 mM $MnCl_2$, 2 mM EDTA, 100 mM Hepes-KOH (pH 8) or 100 mM Bicine (pH 8), 2 mM DTT, 10 mM $NaHCO_3$, 0.1 mM PMFS, 1% v/v Triton, and 2% w/v PPVP. Approximately 1 mL of extraction buffer was used per every 100 mg frozen plant tissue. Prior to centrifugation, an aliquot of the plant extract was added to 100% acetone in a 1 to 4 dilution, to extract chlorophyll in 80% acetone. Samples were keep in the dark at 4˚C (usually 1 d) to extract all the chlorophyll. Extracts were centrifuged at 15,000*g* for 5 min prior to assessment. Chlorophyll concentration was determined using a Perkin-Elmer 552A Spectrophotometer using constants from Porra *et al*. (1989).

Rubisco content was quantified using radiolabeled 2-^{14}C-carboxyarabinitol 1, 5-bisphosphate (^{14}C-CABP) which binds specifically and irreversibly to the RuBP binding site of Rubisco (Zhu and Jensen 1990). The homogenate was centrifuged at 15,000*g* for 1 min, 25 µL of the clear supernatant was added to 100 µL of 0.04 mM ^{14}C-CABP and allowed to incubate for 45 minutes at 25 ˚C. Protein (including ^{14}C -CABP labeled Rubisco) was precipitated with the addition of 125 µL 40% PEG 4000 in 100 mM Hepes-KOH (pH 8) and 25 mM $MgCl_2$ for 10 min at 25 ˚C. The precipitate was centrifuged at 15,000*g* for 5 min and washed with 250 µL 20% PEG 4000 in 20 mM $MgCl_2$, and centrifuged again at 15,000*g* for 5 min to remove unbound

^{14}C-CABP. The pellet was resuspended in 100 μL of resuspension buffer (100 mM Hepes-KOH (pH 8) and 10 mM $MgCl_2$), which was then added to 10 mL of Biodegradable Counting Scintillant cocktail. Radiolabeled ^{14}C was counted with a Tri-Carb 1900 TR Liquid Scintillation Analyzer. Rubisco protein content was calculated assuming 6.5 moles of CABP binding per mol Rubisco, and assuming 560 kD molecular mass of Rubisco (Zhu and Jensen 1990).

Soluble protein was determined in the supernatant of the crude plant extract after 5 min of centrifugation at 15,000*g* and assayed according to the Bradford method (Bradford 1976). Bradford's Regent, which was diluted to 80% strength with water, was added to 5 μL of the plant extract, mixed, and allowed to incubate for 15 min at room temperature. The absorbance was measuring with the aforementioned spectrophotometer at 595 nm. A standard curve with bovine serum albumin (BSA) was used for calibration.

Data analysis.

Data points from CO_2 and light response curves were fitted with two different equations: the nonrectangular hyperbola in accordance with Ögren (1993) and the Mitscherlich equation (Peek *et al.* 2002) using Sigma Plot. The modified nonrectangular hyperbola equation (Eq. (2)) was modified to account for daytime respiration (R_D) which was determined under 0 PPFD during the light response curve.

$$A = \frac{(\phi I + A_{\max}) - \sqrt{(\phi I + A_{\max})^2 - 4\theta\phi I A_{\max}}}{2\theta} - R_D \qquad \text{Eq. (2)}$$

In the equation A is the CO_2 assimilation rate (μmol CO_2 m^{-2} sec^{-1}), ϕ is the maximum incident quantum yield, θ is the convexity factor, *I* is the absorbed PPFD, A_{max} is the maximum assimilation rate, and R_d is dark respiration.

The Mitscherlich model equation is shown below in Eq. (3).

$$A = A_{\max}(1 - e^{-\phi(I-LCP)}) \qquad \text{Eq. (3)}$$

As in Eq. (2), A is the CO_2 assimilation rate (μmol CO_2 m^{-2} sec^{-1}), ϕ is the maximum incident quantum yield, θ is the convexity factor, *I* is the absorbed PPFD, and A_{max} is the maximum assimilation rate. An additional factor is included in the Mitscherlich equation that accounts for the light compensation point, abbreviated LCP. The LCP is the light energy required for the rate of CO_2 assimilation to offset the rate of R_D, resulting in no net CO_2 assimilation.

A two-way ANOVA analysis was performed on several parameters in conjunction with the Tukey test at 95% confidence interval using Minitab® Statistical Software 15.1.0.0 from Minitab Inc., State College, PA.

Light microscopy.

The youngest mature leaves were fixed in 2% (v/v) paraformaldehyde and 1.25% (v/v) gluteraldehyde in 50 mM Pipes buffer, pH 7.2 overnight at 4 ˚C. The samples were dehydrated with a standard ethanol procedure and embedded in London Resin White (LR White, Electron Microscopy Sciences, Fort Washington, PA, USA) acrylic resin. Semi-thin sections (1 μm) were made with Reichert Ultracut R ultramicrotome (Reichert-Jung GMbH, Heidelburg, Germany), dried onto gelatin coated slides, and stained with 1% Toluidine blue O.

Results

Anatomy.

Five different anatomical leaf and cell ultra-structures from the subfamily Suaedoideae are represented in this study: *Salsina* type Kranz C_4, *Schoberia* type Kranz C_4, *Borszczowia* type non-Kranz C_4, *Bienertia* type non-Kranz C_4, and *Brezia* type C_3 (Schütze *et al.* 2003). The two C_4 Kranz-types, *Schoberia*-type and *Salsina*-type anatomies are represented by S. *eltonica* and *S. taxifolia,* respectively. *Suaeda aralocaspica* and *B. sinuspersici* represent *Borszczowia*-type and *Bienertia*-type non-Kranz C_4 anatomies, respectfully. The two C_3 species (*S. heterophylla* and *S. maritima*) both have Brezia-type C_3 anatomy.

Suaeda aralocaspica has a single layer of elongated polarized chlorenchyma cells around the periphery of the leaf. The chlorenchyma cells are very elongated and appear similar to in dimension to Kranz-anatomy in species having *Salsina*-type anatomy except *S. aralocaspica* does not have cell walls separating the chloroplasts that are located at opposite ends of the cell (Fig 1A). To the exterior of the chlorenchyma cells is a hypodermal layer and epidermal layer. The vascular bundles are located interior to the chlorenchyma cells.

Bienertia sinuspersici (Fig 1B) has 1-2 chlorenchyma layers with substantial internal air space directly interior to a tightly connected epidermal layer. Internal to the chlorenchyma cells are large water storage cells that surround the vascular bundles located along the central plane. The most distinctive part of *B. sinuspersici's* anatomy is the chlorenchyma cell ultrastructure, with its conspicuous central cytoplasmic compartment (CCC), in addition to a peripheral layer of chloroplasts.

Salsina (formally known as suaedoid) Kranz C_4 anatomical leaf type is represented in this study by *S. taxifolia* (Fig. 1C). Kranz-anatomy consists of two distinct chlorenchyma tissues; an outer layer of mesophyll cells and an inner layer of Kranz cells (sometimes referred to as bundle sheath cells when surrounding the vascular tissue). In *S. taxifolia,* the mesophyll and Kranz-cells are located around the periphery of the leaf immediately to the interior of the epidermis. The Kranz-cell chloroplasts are located in the centripetal position. The water storage cells just to the interior of the Kranz-cells surround the vascular bundles that lay along the central plane of the leaf.

S. eltonica (C_4) represents the *Schoberia* (formally known as conospermoid) C_4 Kranz anatomical type which is characterized by the mesophyll and Kranz cells located to the interior of a water storage hypodermal layer (Freitag and Stichler 2000; Schütze *et al.* 2003; Voznesenskaya *et al.* 2007). As illustrated in Fig. 1D, the Kranz cell chloroplasts are positioned centrifugally, and the Kranz cell surrounds the vascular bundles which lay along the central plane similar to *Salsina*-type (Freitag and Stichler 2000; Schütze *et al.* 2003).

Both *S. heterophylla* and *S. maritima* are C_3 species which have the *Brezia-type* C_3 anatomy (see Fig. 1E & F, respectfully) (Schütze *et al.* 2003). *Brezia* anatomy is characterized by semiterete leaves with a flatten adaxial side, and with 3-4 layers of chlorenchyma cells that increase in size and decrease in chloroplast content towards the interior. The vascular bundles are located along the central plane curving upwards at the ends. The bundle sheath cells are devoid of chloroplasts, and internal air space (Schütze *et al.* 2003).

Light Response.

The light response curves for all of the species are shown in Fig. 2. The photosynthetic rates in row 1 of Fig. 2 are expressed based on leaf area exposed to incident light, in row 2 rates on a chlorophyll basis, and in row 3 on a Rubisco protein basis. The absorbed quantum for all species in this study is 90% of incident radiation, except for *B. sinuspersici*, which absorbs approximately 75% of the incident radiation. The convexity factor represents the sharpness of the angle between the light limited portion of the response curve and the enzyme or capacity limited portion of the curve (Ögren 1993). Table 1 summarizes the light curve components from the best-fit curves.

The difference in several of the light curve components (ϕ, θ, and LCP) do not appear to correlate with photosynthetic types according to One-way ANOVA tests. The Mitscherlich model was not used to estimate ϕ, because the values were an order of magnitude lower than the ϕ estimates using Eq. (1) and estimates using the initial slope of the points at the lowest light levels. This problem was addressed in the Peek and Russek-Cohen paper (2002), resulting in them rescaling the ϕ values. *Suaeda aralocaspica* has a high incident quantum yield of 0.069 ± 0.004, whereas *S. taxifolia* has the lowest among the C_4 species, $\phi = 0.038 \pm 0.002$. *Suaeda heterophylla* has the lowest ϕ among all the species with $\phi = 0.020 \pm 0.004$. *Suaeda maritima* has a ϕ value of 0.044 ± 0.006 which is intermediate to *S. eltonica* and *B. sinuspersici,* 0.070 ± 0.005 and 0.040 ± 0.002 respectfully (Table 1).

The maximum rates of photosynthesis (A_{max}) tend to be higher among C_4 species than C_3 species expressed per leaf area. One-way ANOVA analysis show at the $P<0.005$ confidence interval that *S. aralocaspica* and *S. eltonica* rates of photosynthesis are significantly higher than *B. sinuspersici* and C_3 species, *S. heterophylla* and *S. maritima.* The photosynthetic rate of *B. sinuspersici* is significantly higher than *S. heterophylla,* but not significantly higher than *S.*

maritima. The photosynthetic rate of *S. taxifolia* is insignificantly different from *S. aralocaspica*, *S. eltonica, B. sinuspersici,* and *S. maritima*, but is significantly greater than *S. heterophylla*. When maximum rates of photosynthesis are expressed per mg chlorophyll (Chl), there were no significant differences between the species (Fig. 2, row 2). However, when the photosynthesis rates are expressed per mg Rubisco (Fig. 2, row 3), *S. aralocaspica* and *B. sinuspersici* have significantly higher rates of photosynthesis than the Kranz-type C_4 species, *S. taxifolia* and *S. eltonica.* All the C_4 species have significantly higher photosynthetic rates than the C_3 on a Rubisco basis.

CO_2 response.

CO_2 response curves are shown in Fig. 3. Same as in the Figure 2, the photosynthetic rates in row 1 of Fig. 3 are expressed as μmol CO_2 fixed per leaf area, in row 2, rates are expressed per milligram of chlorophyll, and in row 3, rates are expressed per milligram of Rubisco protein. All CO_2 response curves for the C_4 species, including single-cell C_4 species, show low CO_2 compensations points, high initial carbon use efficiency, and photosynthesis is saturated near ambient CO_2. This is an obvious contrast to the C_3 species, *S. heterophylla* and *S. maritima*, whose photosynthesis is not saturated even at 1000 μbar CO_2.

The single-cell C_4 species, *B. sinuspersici* and *S. aralocaspica* had low Γ of 15.4 ± 1.4 and 14.6 ± 1.1 μbar CO_2 respectfully. These values were similar to Γ of Kranz-C_4 species *S. eltonica* and *S. taxifolia* with compensation points of 12.4 ± 1.6 and 13.3 ± 0.9 μbar CO_2, respectfully. *Suaeda heterophylla* and *S. maritima* (C_3 species) had Γ points of 74.9 ± 6.1 and 83.9 ± 0.82 μbar CO_2, respectfully, which were significantly higher than any of the C_4 species Γ points. The method described by Brookes and Farquahar (1985) to determine Γ_* without the

contribution of dark-type respiration resulted in lower CO_2 compensation points for all species (Fig. 4). The values of the CO_2 Γ and Γ_* are summarized in Table 2.

The apparent maximum carboxylation efficiency (C_E) is the initial slope of an A/ Ci curve under saturating light. There were significant differences between the C_3 and single-cell C_4 species, with the C_3 species' C_E being significantly lower than the single-cell C_4 species. *Suaeda aralocaspica*'s C_E was not significantly different from the Kranz-type C_4 species, whereas *B. sinuspersici*'s C_E was significantly higher. The results are summarized in Table 2.

The degree of increase in the rate of photosynthesis from current atmospheric levels (~340 μbar) to CO_2 saturated rates (1000 μbar is saturating or near saturating for all species) were measured. Due to the top end limitations of CO_2 external concentrations and the difficultly in determining an exact point of photosynthesis saturation on an external CO_2 level, the increase in photosynthetic rate from 340 μbar CO_2 (ambient CO_2 levels) to 927 μbar CO_2 was used to compare the different photosynthetic types, this is illustrated in Fig. 5. The fold increase in photosynthetic rate was significantly less for C_4 anatomical types (Kranz and single-cell) than for the C_3 species, $P<0.0001$. There was no significant difference between the different C_4 anatomical types (*Bienertia*, *Borszczowia*, *Salsina*, *Brezia,* and *Schoberia*).

Water-use efficiency.

All the C_3 species had significantly lower WUE values than all the C_4 species (Fig. 6). *Bienertia sinuspersici* and *S. taxifolia* had the highest WUE values of 7.9 ± 0.66 and 8.1 ± 0.78 μmol CO_2 fixed per mmol H_2O lost, respectfully. *Suaeda aralocaspica* had slightly, though significantly, lower WUE than *B. sinuspersici* and *S. taxifolia*. WUE for *S. eltonica* was not significantly different from *B. sinuspersici*, *S. taxifolia* or *S. aralocaspica*.

Rubisco Content.

Figure 7 represents the amount of Rubisco in the branches of species expressed as a fraction of the total soluble protein. *Bienertia sinuspersici* and *S. aralocaspica* has significantly lower Rubisco to soluble protein ratios than C_3 species, *S. heterophylla* and *S. maritima*. The Kranz-type C_4 species also had lower Rubisco content than the C_3 species. There was no significant difference between different C_4 anatomical types. Although, there was no significant difference at the 95% confidence interval with the Tukey test among the C_4 species, the average values ranged from 9 to 16 %. The ratios of Rubisco to total soluble protein were lowest in *S. taxifolia* with 0.09 ± 0.02 mg Rubisco per mg soluble protein. Next lowest ratios were *S. aralocaspica* and *B. sinuspersici* with 0.10 ± 0.01 and 0.11 ± 0.02 mg Rubisco per mg soluble protein, respectfully. *Suaeda eltonica* has a slightly higher ratio than the other C_4 species in the comparison with 0.16 ± 0.02 mg Rubisco per mg soluble protein. In both C_3 species, Rubisco was about 30% of the total soluble protein.

Discussion

Since the discovery of the single-cell C_4 pathway, questions have been raised about whether the single-cell terrestrial C_4 photosynthesis systems can be as efficient as the Kranz-type C_4, or whether there may be any specific physiological advantage(s) over the traditional Kranz-type C_4 pathway (Edwards and Walker 1983; Von Caemmerer 2003; von Caemmerer and Furbank 2003). With the recent interest in genetically modifying major C_3 crops to perform C_4 photosynthesis (Ku *et al.* 2001; Long *et al.* 2006; Matsuoka and Sanada 1991; Sheehy *et al.* 2000) there is need to know it is of interest to know if C_4 photosynthesis may be effectively

carried out within a single cell, perhaps reducing the number of steps required to genetically engineer the C_4 pathway in C_3 crops.

In addition to the CO_2 concentrating mechanism, C_4 plants are known to have characteristic features compared to C_3 plants. In addition, it has long been recognized that diffusive resistance to CO_2 leakage out of the Rubisco containing compartment is essential to the efficient function of C_4 photosynthesis (Kiirats *et al.* 2002; von Caemmerer and Furbank 2003). Therefore, it is reasonable to question whether a C_4 pathway which lacks a cell wall between the PEPC CO_2 fixing and the Rubisco CO_2 fixing compartments would significantly reduce the CO_2 diffusive resistance barrier. While, this study does not attempt to quantify the diffusive resistance or leakiness of CO_2 directly, analysis of photosynthetic parameters of *S. aralocaspica* and *B. sinuspersici* can used to evaluate whether greater futile cycle or leakiness is occurring in these species compared to Kranz-type species.

Light Response

The photosynthetic light response curves generally agree with previous C_3 vs. C_4 light responses (see introduction chapter) (Björkman and Berry 1973; Edwards and Walker 1983). In the present study, under 25 ˚C and atmospheric CO_2, there is little difference in ϕ between C_3 and C_4 photosynthesis. Values of ϕ ranged from 0.070 to 0.020 (see Table 2). The efficiency of light energy conversion to chemical energy for CO_2 assimilation is represented by ϕ, or the initial slope at limiting light. The inverse of ϕ is the quantum requirement, which we know from research by Robert Emerson (Govindjee and Govindjee 1999) that the minimum quantum requirement is 8 photons absorbed to produce 3 ATP and 2 NADPH, which is the energy requirement of the C_3 cycle to fix 1 CO_2 fixed, or a maximum ϕ value of 0.125. However, the

maximum ϕ observed in higher plants under atmospheric levels of CO_2 and 25 ˚C is about half of the theoretical maximum (Ehleringer and Björkman 1977; Ehleringer and Pearcy 1983; Lal and Edwards 1995). The reduction of ϕ may be attributed to other processes which utilize assimilatory power, such as photorespiration, and nitrogen assimilation The C_4 cycle requires approx. 2.5 ATP in addition to the energy requirements of the Calvin-Benson cycle, which can be achieved through cyclic electron flow by absorbing 2.5 quanta (Henderson *et al.* 1992). Therefore, the theoretical maximum ϕ (assuming 100% efficiency) in C_4 plants is 0.098 or 10.25 quanta per CO_2 fixed (Lal and Edwards 1995). The relatively high ϕ values of *S. aralocaspica* and *S. eltonica* indicate that the C_4 pathway is functioning efficiently in these species. The lower ϕ of 0.04 found in *B. sinuspersici*, *S. taxifolia*, and *S. maritima* indicates the energy transfer between light absorption and CO_2 assimilation is less efficient in these species. Further tests are required to determine if photorespiration is responsible for the decrease in ϕ in these species.

At high light intensities, C_4 plants typically have higher photosynthetic rates, and their photosynthesis is saturated at higher light intensities than typical C_3 plants (Björkman and Berry 1973; Edwards and Walker 1983). The C_4 species, *S. aralocaspica, S. eltonica,* and *S. taxifolia*, exhibited higher rates of photosynthesis ($P<0.05$) on an area basis than the C_3 species under high light and ambient CO_2 levels at 25 ˚C (Fig. 2). *B. sinuspersici* had the lowest CO_2 assimilation rates (A) per area or per mg chlorophyll basis than any of the other C_4 species in this study. However where A is expressed per Rubisco, the single-cell C_4 species out perform the Kranz-type C_4 species and C_3 species (Fig 2, row 3).

In *B. sinuspersici,* photosynthesis was not fully saturated up to 1700 incident PPFD. Light saturation for *S. aralocaspica* appears relatively low in comparison to the other C_4 species (around 1200 PPFD). Both *S. eltonica* and *S. taxifolia* were light saturated at approx. 1400

incident PPFD. On the other hand, the photosynthetic rate of *S. heterophylla* was saturated at approximately 700 PPFD, which is the lowest intensity of saturation for any plant in the study. *Suaeda maritima* required approx. 1000 PPFD of light to saturate its photosynthesis. The C_3 species appear to have their photosynthesis saturated at lower light intensities than the C_4 species (this study) (Ehleringer and Pearcy 1983; Long and Drake 1991).

All C_4 species have higher photosynthesis rates than C_3 *S. heterophylla (*$P<0.001$). C_4 *Suaeda* species and *B. sinuspersici* can use considerably more light for photosynthesis than C_3 species, *S. heterophylla*. Greater ability to harness light for photosynthesis is a trait of C_4 plants. Single-cell C_4 *S. aralocaspica* has a very high photosynthetic capacity that is nearly double that of the other single-cell C_4 species, *B. sinuspersici*. Despite *B. sinuspersici* having the lowest maximum photosynthetic rate at saturating light of the C_4 species (this study), the light intensity required to saturate photosynthesis are indicative of C_4 and not C_3 or C_3-C_4 intermediate photosynthesis (Björkman and Berry 1973; Edwards and Walker 1983; Ehleringer and Pearcy 1983). There was no statistically significant difference in θ or LCP between species ($P = 0.107$. and $P = 0.180$, respectfully).

CO_2 Response

The CO_2 response curves of the single-cell C_4 species are characteristic of other types of C_4 photosynthesis. It is well known that C_4 species have low CO_2 compensation points, high C_E, and are near saturation at or near current levels of atmospheric levels of CO_2 (~340 μbar) (Björkman and Berry 1973; Edwards and Walker 1983; Sage 1999).

C_4 species in general have higher C_E values than C_3 species. This is because C_4 species not are inhibited by high concentrations of O_2 and the catalytic frequency of Rubisco is higher in

C_4 than in C_3 species (Wessinger *et al.* 1989). The most accurate method to calculate C_E is to determine the soluble fraction of CO_2, which gives a measurement of the actual CO_2 available to Rubisco (Ku and Edwards 1977). The C_E values in this study were based off external CO_2 concentrations, which may under estimate the true C_E. The soluble CO_2 concentration should be used to determine the true C_E. The C_E of the C_4 species in this study was significantly higher ($P<0.001$) than the C_E in the C_3 species (3-4 folds) (Table 2). Since the C_E is primarily inhibited by competitive inhibition from O_2, the high C_E among the single-cell C_4 species indicates a functional and efficient C_4 pathway.

Values for Γ were higher than expected for both C_3 and C_4 species. Typical Γ values for C_4 species is near 1-10 μbar CO_2 and 40+ μbar CO_2 for C_3 plants (Krenzer *et al.* 1975). The higher Γ values (this study, Table 2) may be due to the presence of a considerable amount of stem. The stems of the species in this study have little to no photosynthetic tissue and may contribute to the evolution of CO_2 through processes other than photorespiration, i.e. normal mitochondrial respiration (Boyd *et al.* 2007; Brooks and Farquhar 1985). The values of Γ_* from this study (Table 2) are more typical of previously published values for other C_4 and C_3 species (Krenzer *et al.* 1975; Sage 1999).

A considerable increase in A from atmospheric CO_2 to elevated CO_2 was observed in all the C_4 species in this study (~ 35%) (this study, Fig. (5). While the increase in A was less than that observed in C_3 species ($P<0.001$), the increase in C_4 species may possibly indicate some limitation of CO_2 fixation. Stomatal resistance could account for the apparent increase in C_4 species. As the external CO_2 concentrations increase, so does the stomatal resistance, which reduces the intercellular CO_2 concentrations (data not shown). The stomatal response to CO_2 is well characterized and is similar among C_3 and C_4 species (Morison and Gifford 1983).

Rubisco Content

Typically, C_4 plants invest less protein into Rubisco, than C_3 plants (Sage *et al.* 1987; Seemann *et al.* 1984). The reason for this is Rubisco in C_4 plants is operating near saturating levels of CO_2 at atmospheric levels of CO_2, because of the CO_2 concentrating mechanism. Rubisco in C_3 plants is operating far below maximum capacity under atmospheric CO_2 conditions, so in order for C_3 plants to achieve high rates of photosynthesis, C_3 plants must invest approx. 30% of their soluble protein into Rubisco (Ku *et al.* 1979; Sage *et al.* 1987; Seemann *et al.* 1984; Von Caemmerer 2003). Both single-cell C_4 types, *B. sinuspersici* and *S. aralocaspica*, show this general trend in our study (Fig. 7).

Since C_4 plants require less Rubisco than C_3 plants to achieve high rates of photosynthesis (Von Caemmerer 2003), it was expected that the C_4 species would have higher photosynthetic rates on a Rubisco basis than C_3 species under atmospheric CO_2. The difference in photosynthetic rates on a Rubisco basis between the single-cell C_4 and Kranz-type C_4 species found in our study was unexpected. Reasons for the increase in A per Rubisco in the single-cell C_4 species compared to Kranz-type C_4 species is not clear. It has been previously shown that *B. cycloptera* and *S. aralocaspica* have a greater ratio of PEPC to Rubisco activity than *Salsola laricina* (a related Kranz-type C_4 species) (Voznesenskaya *et al.* 2002; Voznesenskaya *et al.* 2001). Perhaps, the ratio of C_4 enzymes to C_3 enzymes is optimized in these single-cell C_4 species to reduce leakage and maximize CO_2 fixation (Sage 2002). It has also been shown that *S. aralocaspica* and *B. cycloptera*, have higher Rubisco enzyme activity than *S. laricina* (Voznesenskaya *et al.* 2002; Voznesenskaya *et al.* 2001), while this study shows that *S. aralocaspica* and *B. sinuspersici* have similar amounts of Rubisco enzyme in comparison to

other Kranz-type C_4 species. More research is needed to determine if there are any kinetic differences in Rubisco between the single-cell C_4 species and Kranz-type C_4 species.

While all the single-cell C_4 species have similar amounts of Rubisco (% of total soluble protein) to their Kranz-type C_4 counterparts, the single-cell C_4 species have proportionally less Rubisco and less protein per leaf area. *S. aralocaspica* and *B. sinuspersici* are both highly succulent (more so than any of the comparative species in this study) which may account for the larger surface area and lower protein levels. If these species have lower nitrogen content per unit leaf area, it could be of interest to determine their nitrogen-use-efficiency and whether they are adapted to live in areas with low nitrogen availability.

Conclusion

The results from this study clearly demonstrate that both single-cell C_4 species are functioning similarly to their Kranz-type C_4 counterparts. Despite the single-cell C_4 species lacking a cell wall as a barrier between fixation of atmospheric CO_2 into C_4 acids, and the donation of CO_2 from the C_4 acids to Rubisco, both *S. aralocaspica* and *B. sinuspersici* appear to have an efficient C_4 cycle with minimal leakage. The single-cell C_4 species have similar WUE, similar Rubisco content (% of soluble protein), CO_2 compensation points, C_E, and similar increases in photosynthetic rate from ambient to 927 μbar CO_2 levels compared to the Kranz-type C_4 species included in this study. Like Kranz-type C_4 species, *S. aralocaspica* and *B. sinuspersici* are distinct from the C_3 species. This further supports the claim that C_4 photosynthesis does not require Kranz-anatomy to operate efficiently.

Acknowledgment

This work was supported by NSF grant IBN-0131098 and NSF grant IBN-0236959, and Civilian Research and Development Foundation Grant RB1-2502-ST-03. We thank the Washington State University EM Center for use of their facilities and staff assistance.

References

Akhani H, Barroca J, Koteeva N, Voznesenskaya E, Franceschi V, Edwards G, Ghaffari SM, Ziegler H (2005) *Bienertia sinuspersici* (Chenopodiaceae): A new species from southwest Asia and discovery of a third terrestrial C4 plant without Kranz anatomy. *Systematic Botany* 30, 290-301.

Akhani H, Trimborn P, Ziegler H (1997) Photosynthetic pathways in Chenopodiaceae from Africa, Asia and Europe with their ecological, phytogeographical and taxonomical importance. *Plant Systematics and Evolution* 206, 187-221.

Bender MM (1971) Variations in the 12C/12C ratios of plants in relation to the pathway of photosynthetic carbon dioxide fixation. . *Phytochemistry* 10, 1239-44.

Berry J, Björkman O (1980) Photosynthetic response and adaptation to temperature in higher plants. *Ann. Rev. Plant Physiol.* 31
491-543.

Björkman O, Berry J (1973) High efficiency photosynthesis. *Sci. Am.* 229, 80 - 90.

Bowes G, Ögren WL, Hageman RH (1971) Phosphoglycolate production catalyzed by ribulose diphosphate carboxylase. *Biochem Biophys Res Commun* 45, 716-22.

Boyd CN, Franceschi VR, Chuong SDX, Akhani H, Kiirats O, Smith M, Edwards GE (2007) Flowers of Bienertia cycloptera and Suaeda aralocaspica (Chenopodiaceae) complete the life cycle performing single-cell C-4 photosynthesis. *Functional Plant Biology* 34, 268-281.

Bradford MM (1976) A rapid and sensitive method for the quantification of microgram quantities of protein utilizing the principle of protein-dye binding. *Analytical Biochemistry* 72, 248-254.

Brooks A, Farquhar GD (1985) Effect of temperature on the CO2/O2 specificity of ribulose-1,5-bisphosphate carboxylase/oxygenase and the rate of respiration in the light. *Planta* 165, 397-406.

Chuong SD, Franceschi VR, Edwards GE (2006) The cytoskeleton maintains organelle partitioning required for single-cell C4 photosynthesis in Chenopodiaceae species. *Plant Cell* 18, 2207-23.

Edwards G, Walker D (1983) 'C3, C4 : Mechanisms, and Cellular and Environmental Regulation of Photosynthesis.' (Blackwell Scientific Publications: Oxford)

Edwards GE, Franceschi VR, Ku MSB, Voznesenskaya EV, Pyankov VI, Andreo CS (2001a) Compartmentation of photosynthesis in cells and tissues of C4 plants. *J. Exp. Bot.* 52, 577-590.

Edwards GE, Franceschi VR, Voznesenskaya EV (2004) Single-cell C4 photosynthesis versus the dual-cell (Kranz) paradigm. *Annual Review of Plant Biology* 55, 173.

Edwards GE, Furbank RT, Hatch MD, Osmond CB (2001b) What does it take to be C4? Lessons from the evolution of C4 photosynthesis. *Plant Physiol* 125, 46-9.

Ehleringer J, Björkman O (1977) Quantum yields for CO2 uptake in C3 and C4 plants: dependence on temperature, CO2, and O2 concentration. *Plant Physiol.* 59, 86-90.

Ehleringer J, Pearcy RW (1983) Variation in quantum yield for CO2 uptake among C3 and C4 plants. *Plant Physiol.* 73, 555-559.

Forrester ML, Krotkov G, Nelson CD (1966) Effect of oxygen on photosynthesis, photorespiration and respiration in detached leaves. I. Soybean. *Plant Physiol.* 41, 422-427.

Freitag H, Stichler W (2000) A remarkable new leaf type with unusual photosynthetic tissue in a central Asiatic genus of Chenopodiaceae. *Plant Biology* 2, 154-160.

Freitag H, Stichler W (2002) *Bienertia cycloptera* Bunge ex Boiss., Chenopodiaceae, another C4 plant without Kranz tissues. *Plant Biology* 4, 121-131.

Govindjee, Govindjee (1999) On the requirement of minimum number of four versus eight quanta of light for the evolution of one molecule of oxygen in photosynthesis: A historical note. *Photosynthesis Research* 59, 249-254.

Hatch M (2002) C4 photosynthesis: discovery and resolution. *Photosynthesis Research* 73, 251-256.

Hatch MD, Slack CR (1966) Photosynthesis by sugarcane leaves. A new carboxylation reaction and the pathway of sugar formation. *Biochem. J.,* 101, 103-111.

Hatch MD, Slack CR (1970) 'The C4-carboxylic acid pathway of photosynthesis. In Progress in Photochemistry.' (Wiley Interscience: London)

Henderson SA, Caemmerer SV, Farquhar GD (1992) Short-term measurements of carbon isotope discrimination in several C4 species. *Functional Plant Biology* 19, 263-285.

Idle DB, Proctor C (1983) An integrating sphere leaf chamber. *Plant, Cell and Environment* 6, 337-440.

Kapralov MV, Akhani H, Voznesenskaya EV, Edwards G, Franceschi V, Roalson EH (2006) Phylogenetic relationships in the Salicornioideae / Suaedoideae / Salsoloideae s.1. (Chenopodiaceae) Clade and a clarification of the phylogenetic position of *Bienertia* and *Alexandra* using multiple DNA sequence datasets. *Systematic Botany* 31, 571.

Kiirats O, Lea PJ, Franceschi VR, Edwards GE (2002) Bundle sheath diffusive resistance to CO2 and effectiveness of C4 photosynthesis and refixation of photorespired CO2 in a C4 cycle mutant and wild-type *Amaranthus edulis*. *Plant Physiol.* 130, 964-976.

Kortschack HP, Hartt CE, Burr GO (1965) Carbon dioxide fixation in sugarcane leaves. *Plant Physiol* 40, 209-213.

Krenzer EG, Jr., Moss DN, Crookston RK (1975) Carbon dioxide compensation points of flowering plants. *Plant Physiol.* 56, 194-206.

Ku MS, Cho D, Li X, Jiao DM, Pinto M, Miyao M, Matsuoka M (2001) Introduction of genes encoding C4 photosynthesis enzymes into rice plants: physiological consequences. *Novartis Found Symp* 236, 100-11; discussion 111-6.

Ku MSB, Schmitt MR, Edwards GE (1979) Quantitative determination of RuBP carboxylase-oxygenase protein in leaves of several C3 and C4 plants. *J. Exp. Bot.* 30, 89-98.

Ku S-B, Edwards GE (1977) Oxygen inhibition of photosynthesis: II. Kinetic characteristics as affected by temperature. *Plant Physiol.* 59, 991-999.

Lal A, Edwards GE (1995) Maximum quantum yields of O2 evolution in C4 plants under high CO2. *Plant Cell Physiol.* 36, 1311-1317.

Landsberg JJ, Ludlow MM (1970) A technique for determining resistance to mass transfer through the boundary layers of plants with complex structure. *Journal of Applied Ecology* 7, 187.

Lara MV, Chuong SD, Akhani H, Andreo CS, Edwards GE (2006) Species having C4 single-cell-type photosynthesis in the Chenopodiaceae family evolved a photosynthetic phosphoenolpyruvate carboxylase like that of Kranz-type C4 species. *Plant Physiol* 142, 673-84.

Long SP, Drake BG (1991) Effect of the Long-Term Elevation of CO2 Concentration in the Field on the Quantum Yield of Photosynthesis of the C3 Sedge, Scirpus olneyi. *Plant Physiol.* 96, 221-226.

Long SP, Xin-Guang Z, Naidu SL, Ort DR (2006) Can improvement in photosynthesis increase crop yields? *Plant, Cell & Environment* 29, 315.

Matsuoka M, Sanada Y (1991) Expression of photosynthetic genes from the C4 plant, maize, in tobacco. *Mol Gen Genet* 225, 411-9.

Morison JIL, Gifford RM (1983) Stomatal sensitivity to carbon dioxide and humidity: a comparison of two C3 and two C4 grass species. *Plant Physiol.* 71, 789-796.

Ögren E (1993) Convexity of the photosynthetic light-response curve in relation to intensity and direction of light during growth. *Plant Physiology* 101, 1013-1019.

Ögren WL, Bowes G (1971) Ribulose diphosphate carboxylase regulates soybean photorespiration. *Nat New Biol* 230, 159-60.

Peek MS, Russek-Cohen E, Wait DA, Forseth IN (2002) Physiological response curve analysis using nonlinear mixed models. *Oecologia* 132, 175-180.

Porra RJ, Thompson WA, Kriedemann PE (1989) Determination of accurate extinction coefficients and simultaneous equations for assaying chlorophylls a and b extracted with four different solvents: verification of the concentration of chlorophyll standards by atomic absorption spectroscopy. *Biochimica et Biophysica Acta* 975, 384-394.

Rasband WS (1997-2007) ImageJ. In. (U. S. National Institutes of Health, Bethesda: Maryland, USA)

Sage RF (1999) 'C4 plant Biology.' (Academic Press)

Sage RF (2002) C4 photosynthesis in terrestrial plants does not require Kranz anatomy. *Trends in Plant Science* 7, 283-285.

Sage RF, Pearcy RW, Seemann JR (1987) The nitrogen use efficiency of C3 and C4 plants : III. Leaf nitrogen effects on the activity of carboxylating enzymes in *Chenopodium album* (L.) and *Amaranthus retroflexus* (L.). *Plant Physiol.* 85, 355-359.

Schütze P, Freitag H, Weising K (2003) An integrated molecular and morphological study of the subfamily Suaedoideae Ulbr. (Chenopodiaceae). *Plant Systematics & Evolution* 239, 257.

Seemann JR, Badger MR, Berry JA (1984) Variations in the specific activity of Ribulose-1,5-bisphosphate carboxylase between species utilizing differing photosynthetic pathways. *Plant Physiol.* 74, 791-794.

Sheehy JE, Mitchell PL, Hardy B (2000) 'Redesigning Rice Photosynthesis to Increase Yield.' (IRRI and Elsevier Science: Makati City, Philippines)

Taiz L, Zeiger E (1998) 'Plant physiology.' (Sinauer Associates: Sunderland, Mass.)

Von Caemmerer S (2003) C4 photosynthesis in a single C3 cell is theoretically inefficient but may ameliorate internal CO2 diffusion limitations of C3 leaves. *Plant, Cell & Environment* 26, 1191-1197.

von Caemmerer S, Furbank RT (2003) The C4 pathway: an efficient CO2 pump. *Photosynth Res* 77, 191-207.

Voznesenskaya EV, Chuong SD, Koteyeva NK, Franceschi VR, Freitag H, Edwards GE (2007) Structural, biochemical, and physiological characterization of C4 photosynthesis in species having two vastly different types of Kranz anatomy in genus *Suaeda* (Chenopodiaceae). *Plant Biol (Stuttg)*.

Voznesenskaya EV, Edwards GE, Kiirats O, Artyusheva EG, Franceschi VR (2003) Development of biochemical specialization and organelle partitioning in the single-cell C4

system in leaves of *Borszczowia aralocaspica* (Chenopodiaceae). *American Journal of Botany* 90, 1669-1680.

Voznesenskaya EV, Franceschi VR, Kiirats O, Artyusheva EG, Freitag H, Edwards GE (2002) Proof of C4 photosynthesis without Kranz anatomy in *Bienertia cycloptera* (Chenopodiaceae). *Plant J* 31, 649-62.

Voznesenskaya EV, Franceschi VR, Kiirats O, Freitag H, Edwards GE (2001) Kranz anatomy is not essential for terrestrial C4 plant photosynthesis. *Nature* 414, 543-6.

Voznesenskaya EV, Koteyeva NK, Chuong SDX, Akhani H, Edwards GE, Franceschi VR (2005) Differentiation of cellular and biochemical features of the single-cell C4 syndrome during lead development *Bienertia cycloptera* (Chenopodiaceae). *American Journal of Botany* 92, 1784.

Wessinger ME, Edwards GE, Ku. MSB (1989) Quantity and kinetic properties of ribulose 1,5-bisphosphate carboxylase in C3, C4, and C3-C4 intermediate species of Flaveria (Asteraceae). *Plant Cell Physiol.* 30, 665-671.

Zhu G, Jensen RG (1990) Status of the substrate binding sites of Ribulose bisphosphate carboxylase as determined with 2-C-carboxyarabinitol 1,5-bisphosphate. *Plant Physiol* 93, 244-249.

Table 1. Light response curve parameters. The quantum yield is represented by ϕ, θ is the convexity factor, A_{max} is the theoretical maximum rate of photosynthesis, R_D is the daytime respiration, and LCP is the light compensation point. Values are in bold while the standard errors of the mean are in parentheses. [1]μmol CO_2 m^{-2} sec^{-1}, [2]μmol quanta m^{-2} sec^{-1}, * represents values with P>0.005, indicating insignificant estimates.

	Suaeda aralocaspica	*Bienertia sinuspersici*	*Suaeda eltonica*	*Suaeda taxifolia*	*Suaeda heterophylla*	*Suaeda maritima*
ϕ	0.069 ± 0.004	0.040 ± 0.002	0.070 ± 0.005	0.038 ± 0.002	0.020 ± 0.004)	0.044 ± 0.006
θ	0.79 ± 0.06	0.64 ± 0.08	0.79 ± 0.07	0.79 ± 0.07	0.95 ± 0.06	0.67* ± 0.23
A_{max}[1]	39 ± 1.2	29 ± 1.3	38 ±1.6	35 ± 1.9	9 ± 0.6	23 ± 1.6
R_D[1]	1.6 ± 0.39	2.1 ± 0.11	2.4 ± 0.37	2.6 ± 0.36	1.2 * ± 0.40	0.84 * ± 2.27
LCP[2]	28 ± 4.0	74 ± 2.7	51 ± 4.7	79 ± 7.0	49 ± 10.9	19 ± 7.5

Table 2. Summary of photosynthetic components relating to CO_2. Γ and Γ_* are the CO_2 compensation points with and without daytime mitochondrial respiration, respectfully. C_E is the carboxylation efficiency. Sat. CO_2 is the concentration of external CO_2 that saturates photosynthesis. The standard error of the mean is included in the parentheses below the mean. Photosynthesis parameters were measured under 1000 PPFD, and 12 mbar H_2O vapor, except of Γ_*. Saturating CO_2, Γ_* and Γ are expressed in µbar. [1]CO_2 fixed per µbar CO_2. [2]A(µmol CO_2 m^{-2} sec^{-1}). [3] Voznesenskaya, Franceschi *et al.* 2001. [4]Akhani, Barroca *et al.* 2005. [5] Akhani, Trimborn *et al.* 1997. [6] Unpublished data.

	Suaeda aralocaspica	*Bienertia sinuspersici*	*Suaeda taxifolia*	*Suaeda eltonica*	*Suaeda heterophylla*	*Suaeda maritima*
Γ	14.6 ± 1.1	15.4 ±1.4	13.3 ± 0.9	12.4 ±1.6	74.9 ± 6.1	83.9 ± 0.82
Γ_*	~3	~5	~2.5	~6	~32	~32
C_E[1]	0.24 ± 0.02	0.41 ± 0.05	0.24 ± 0.01	0.21 ± 0.02	0.06 ± 0.003	0.08 ± 0.013
$\triangle^{13}C$ (‰)	-12.4[3]	-13.9[4]	-12.2[6]	-14.2[6]	-29.6[6]	-27.4[5]
Sat. CO_2	~500	~650	~300	~500	>1000	>1000
A_{MAX}[2] (Amb. CO_2)	35 ± 0.6	20 ±0.9	26 ± 0.7	26 ± 3.4)	7 ±1.3	18 ± 0.2
A_{MAX}[2] (High CO_2)	38± 2.2	20 ± 0.8	26 ± 4.0)	26 ± 0.8	17 ± 0.8	49 ± 0.7

Figure 1. Cross sections. A.) *S. aralocaspica* with borszczoviod anatomy, B.) *B. sinuspersici* with bienertioid single-cell C_4 anatomy, C.) *S. taxifolia* with *Salsina*-type C_4 anatomy, D *S. eltonica* with conospermoid C_4 Kranz-anatomy, E.) *S. heterophylla* with Brezia C_3 anatomy, and F.) *S. maritima* with *Brezia* C_3 anatomy. M = Mesophyll cells, B = Bundle sheath or Kranz cells, V = vascular bundles. Scale bar = 100 μm.

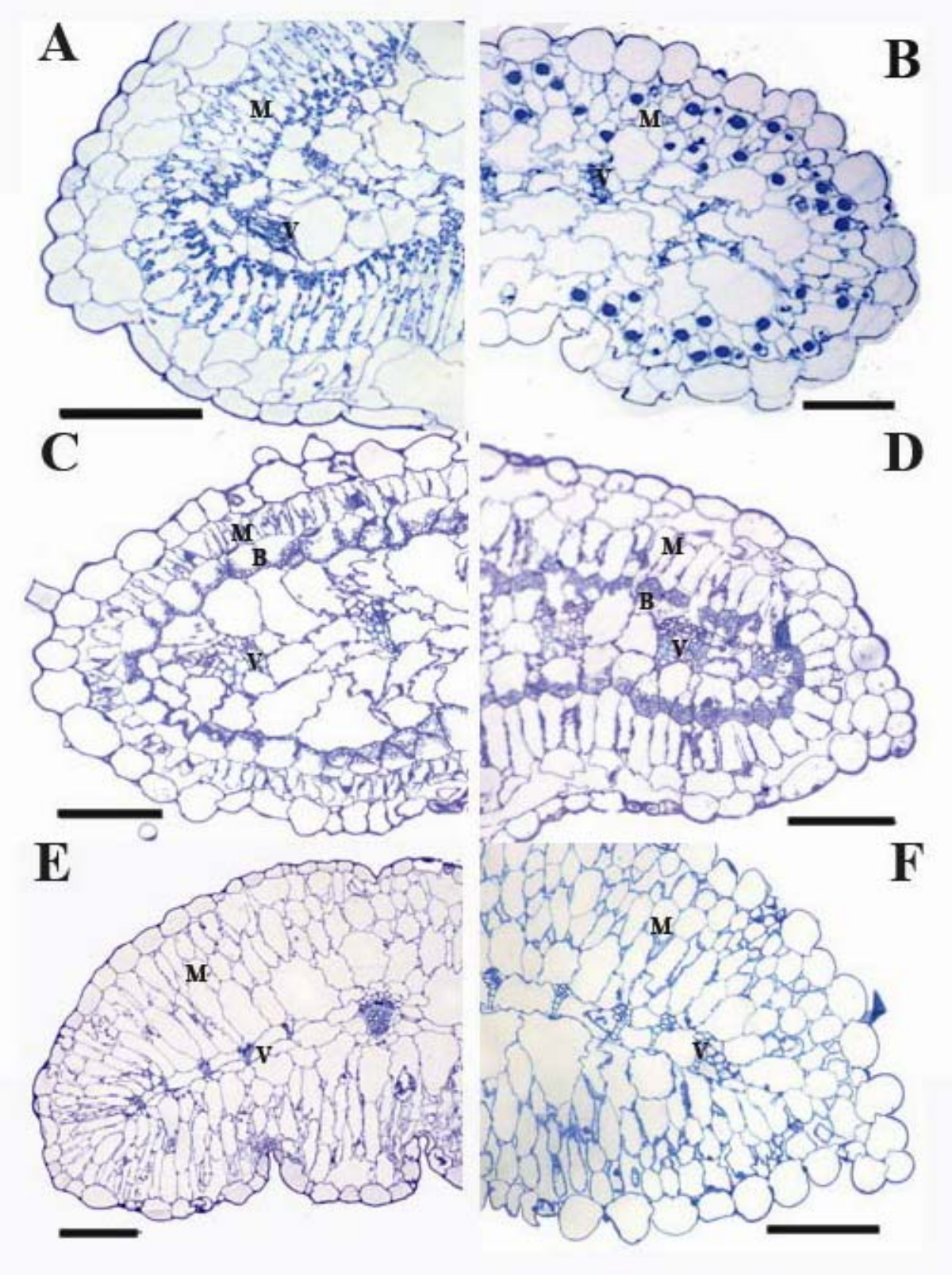
A
M
V
B
M
V
C
M
B
V
D
M
B
V
E
M
V
F
M
V

Figure 2. Light response curves. The single-cell C_4 species, ●*S. aralocaspica* and ○ *B. sinuspersici* are represented in column 1. Kranz-type C_4 species, ▲ *S. taxifolia* and △ *S. eltonica,* are represented in column 2. C_3 species, ■ *S. heterophylla* and □ *S. maritima* are represented by column 3. The photosynthetic rates in row 1 are expressed μmol CO_2 fixed per leaf area, in row 2, rates are expressed per milligram of chlorophyll, and in row 3, rates are expressed per milligram of Rubisco protein. The error bars represent the standard error of the mean. N= 3

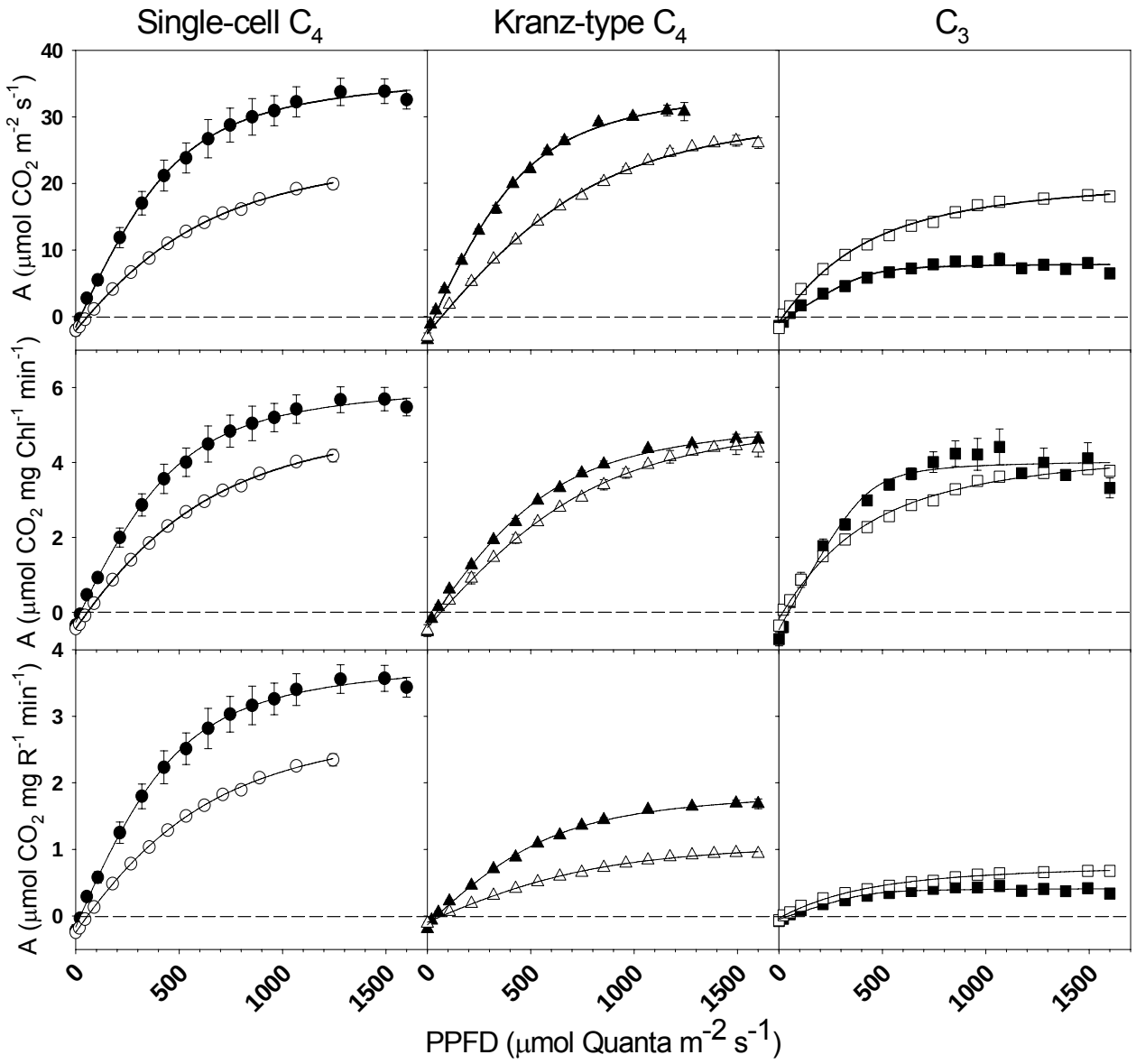
Single-cell C4
Kranz-type C4
C3
A (μmol CO2 m-2 s-1)
A (μmol CO2 mg Chl-1 min-1)
A (μmol CO2 mg R-1 min-1)
PPFD (μmol Quanta m-2 s-1)

Figure 3. CO_2 response curves. The single-cell C_4 species, ●*S. aralocaspica* and ○ *B. sinuspersici* are represented in column 1. Kranz-type C_4 species, ▲ *S. taxifolia* and △ *S. eltonica,* are represented in column 2. C_3 species, ■ *S. heterophylla* and □ *S. maritima* are represented by column 3. The photosynthetic rates in row 1 are expressed in μmol CO_2 fixed per leaf area, in row 2, rates are expressed per milligram of chlorophyll, and in row 3, rates are expressed per milligram of Rubisco protein. All CO_2 response curves for the C_4 species, including single-cell C_4 species, show low CO_2 compensations points, high initial carbon use efficiency, and photosynthesis is saturated near ambient CO_2. This is an obvious contrast to the C_3 species, *S. heterophylla*, whose photosynthesis is not saturated even at 927 μbar CO_2. N=3

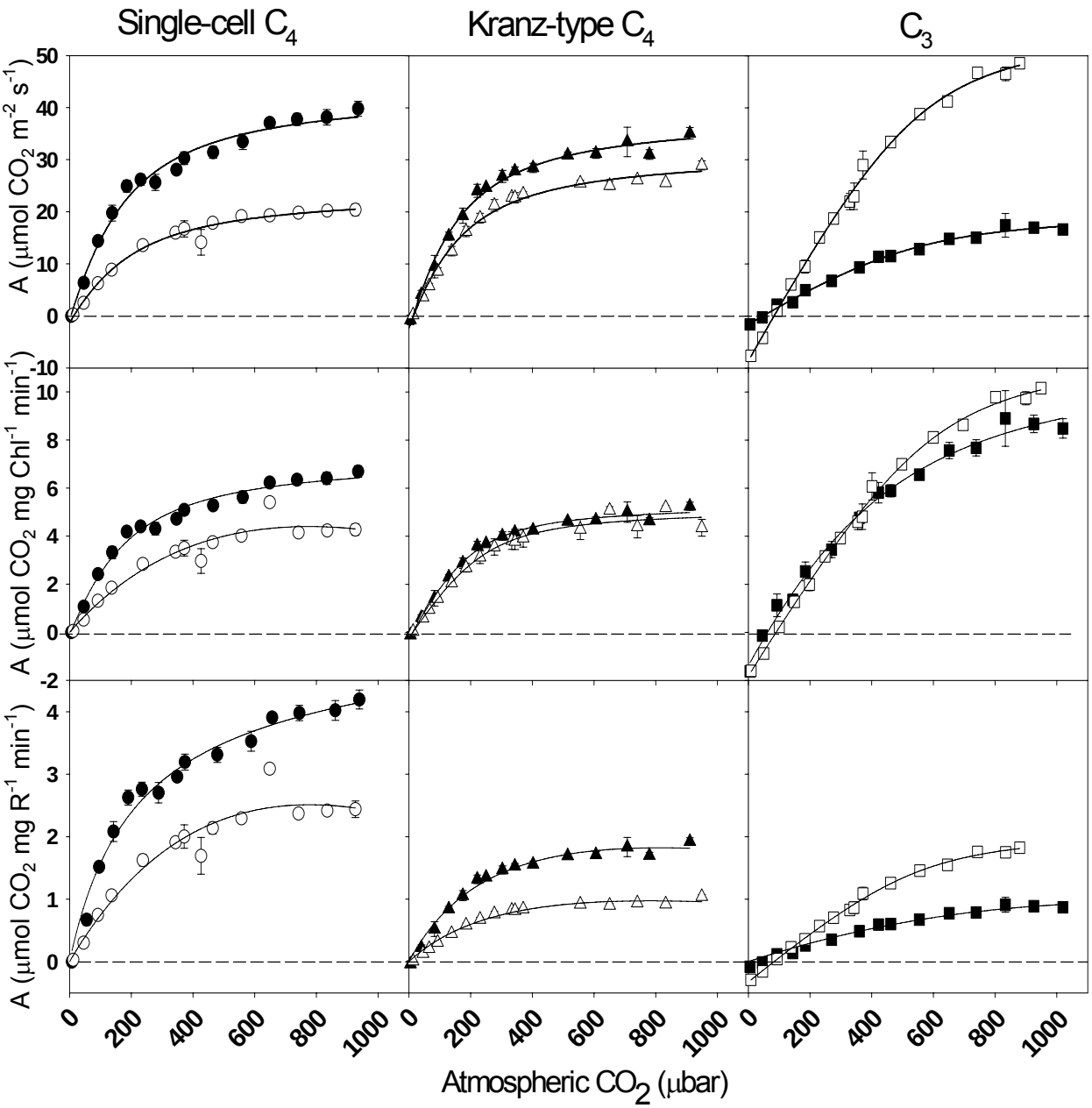
Single-cell C_4
Kranz-type C_4
C_3
A (μmol CO_2 m^{-2} s^{-1})
A (μmol CO_2 mg Chl^{-1} min^{-1})
A (μmol CO_2 mg R^{-1} min^{-1})
Atmospheric CO_2 (μbar)

Figure 4. Determination of Γ_*. Γ* is the point where the net exchange of CO_2 would be zero if there were no CO_2 evolution from processes other than photorespiration. This can be determined by extrapolation to the x-axis the point where photosynthesis is invariant to light, indicated by the point where all the lines cross. This point was determined by measuring CO2 response curves at low light intensities. At that point the CO_2 concentration is Γ*, and the CO_2 exchange rate is equal to R_D. Γ* is considered to be a more accurate indicator of the CO_2 compensation point based on Rubisco carboxylase versus oxygenase activity.

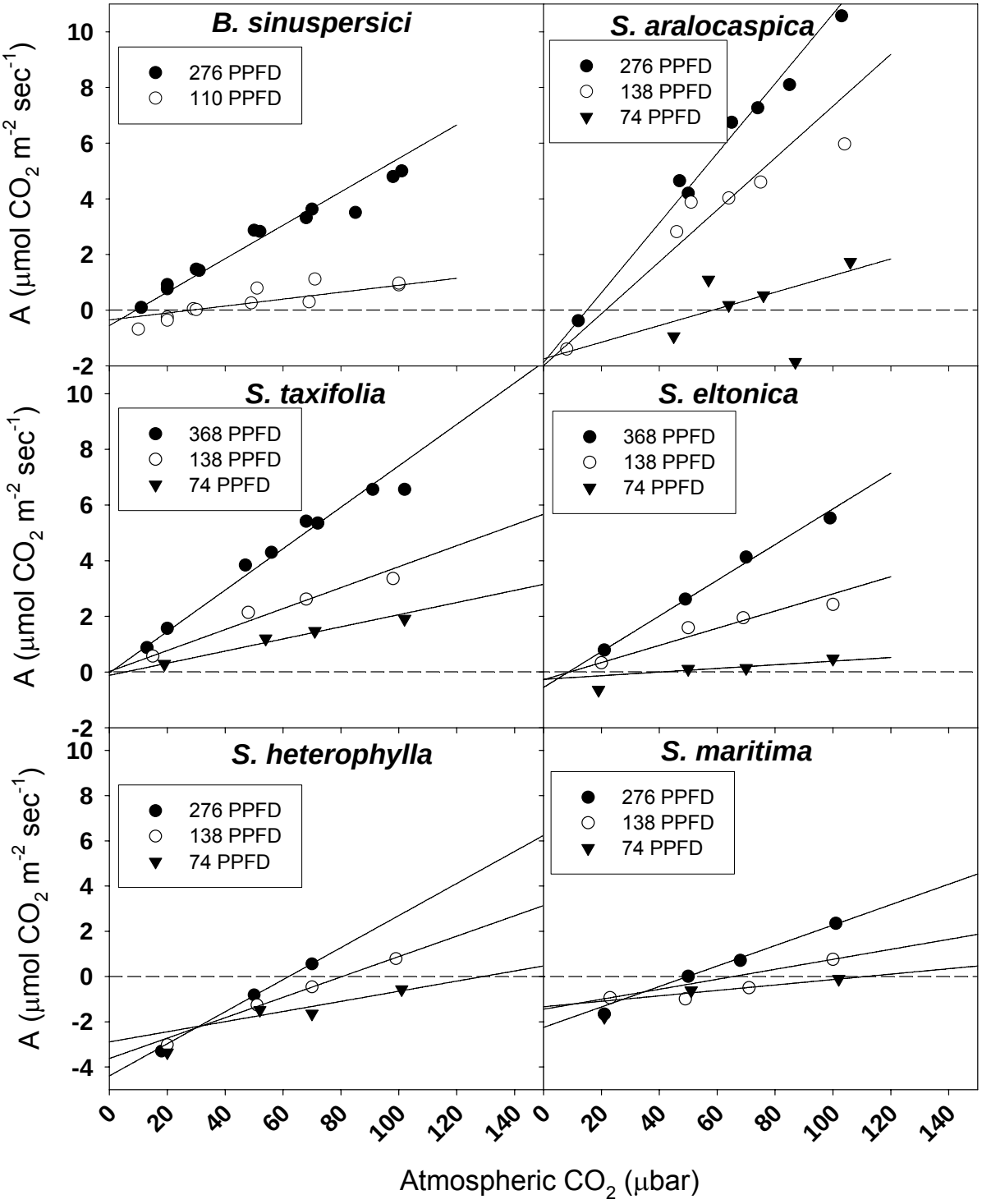
B. sinuspersici
276 PPFD
110 PPFD
S. aralocaspica
276 PPFD
138 PPFD
74 PPFD
S. taxifolia
368 PPFD
138 PPFD
74 PPFD
S. eltonica
368 PPFD
138 PPFD
74 PPFD
S. heterophylla
276 PPFD
138 PPFD
74 PPFD
S. maritima
276 PPFD
138 PPFD
74 PPFD
A (μmol CO2 m-2 sec-1)
Atmospheric CO2 (μbar)
10
8
6
4
2
0
-2
-4
0
20
40
60
80
100
120
140

Figure 5. Graph of the percentage increase in photosynthetic rates when atmospheric CO_2 is increased from 340 µbar CO_2 to 927 µbar CO_2. Measurements were under 1000 PPFD, 25˚C, and 12 mbars H_2O vapor. The error bars represent the standard of the mean (N=3). Two-way ANOVA tests were done to determine the significance. The photosynthetic rates of C_3 species nearly doubled from ambient CO_2 (340 µbar) to elevated CO_2 (927 µbar CO_2) which is significantly higher than the C_4 species. Different letters represent significant differences; the same letter indicates so significant difference based on $P<0.001$.

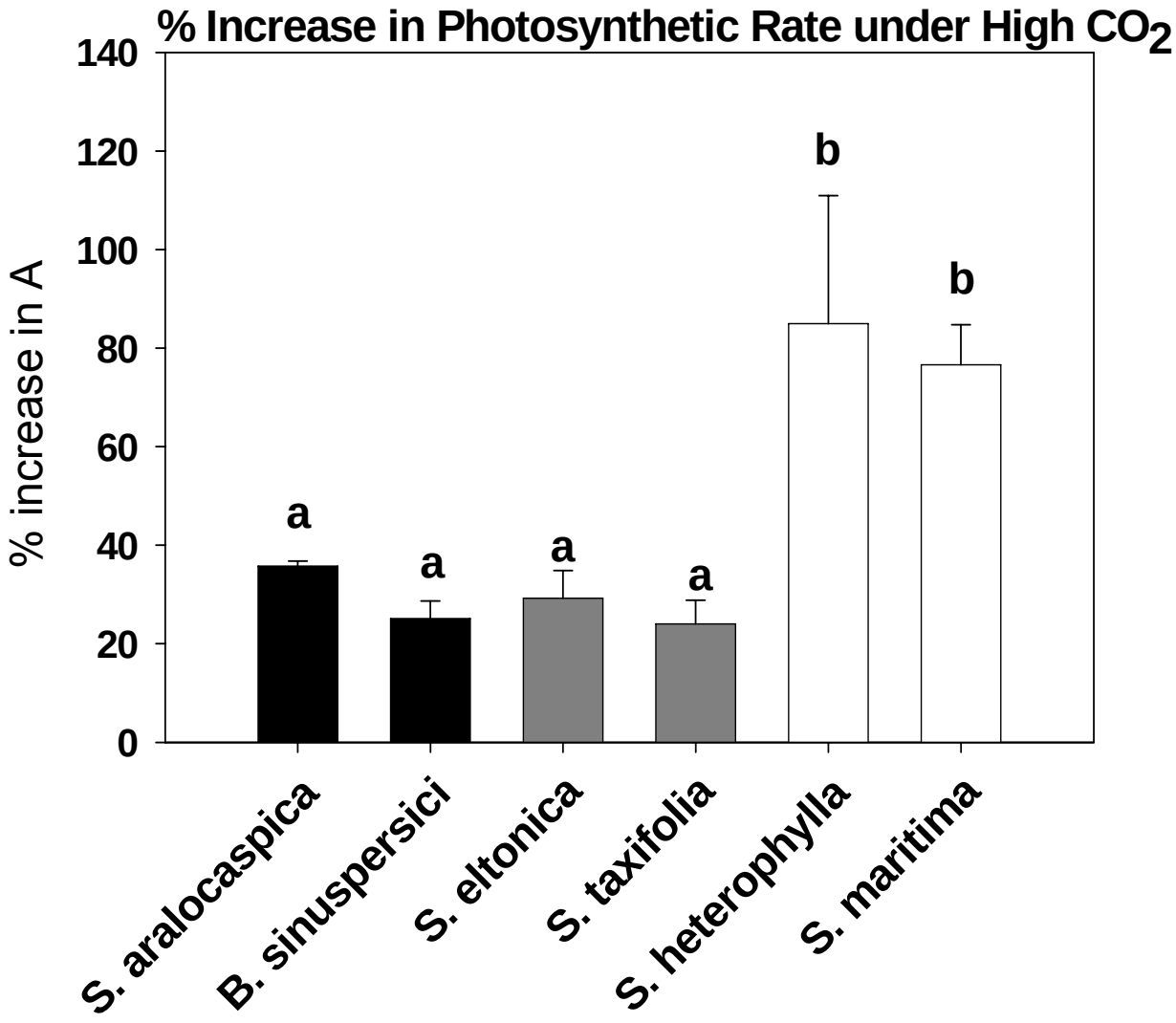

Figure 6. Measurements were under 1000 PPFD, 25˚C, and 12 mbars H_2O vapor. The error bars represent the standard of the mean. Two-way ANOVA tests were done to determine the significance. The C_3 species have a significantly lower WUE than the C_4 species. Different letters represent significant differences; the same letter indicates so significant difference based on $P<0.001$. N=3

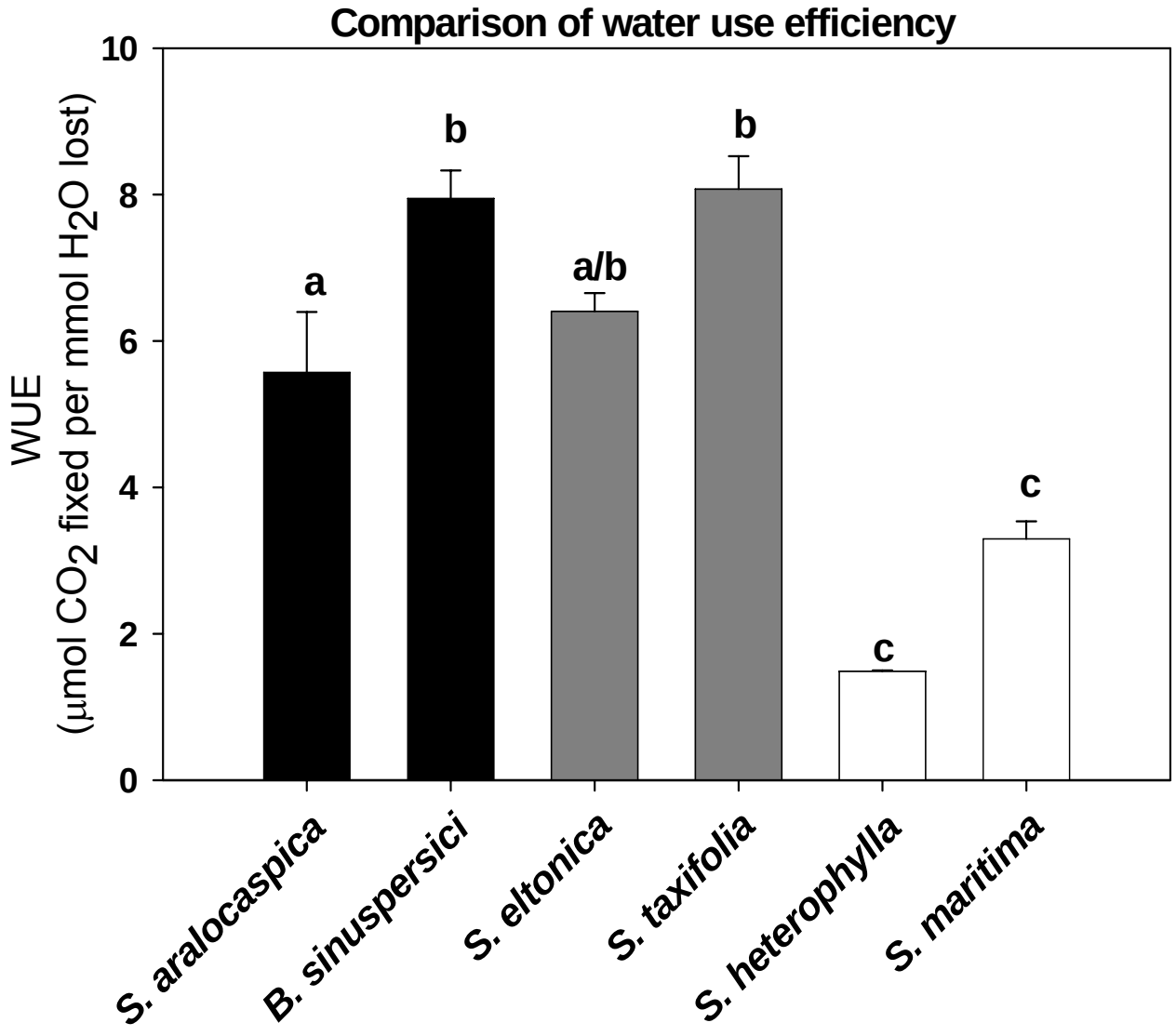

Figure 7. Rubisco content is expressed in mg Rubisco protein per mg soluble protein. The error bars represent the standard of the mean. Two-way ANOVA tests were done to determine the significance. The C_3 have a significantly higher Rubisco content than the C_4 species. Different letters represent significant differences; the same letter indicates so significant difference based on $P<0.001$. N=3